

Quantum dynamics of electronic excitations in biomolecular chromophores: role of the protein environment and solvent

Joel Gilmore and Ross H. McKenzie*

Department of Physics, University of Queensland, Brisbane 4072 Australia

June 22, 2019

Abstract

We consider continuum dielectric models as minimal models to understand the effect of the surrounding protein and solvent on the quantum dynamics of electronic excitations in a biological chromophore. For these models we describe expressions for the frequency dependent spectral density which describes the coupling of the electronic levels in the chromophore to its environment. We find the contributions to the spectral density from each component of the chromophore environment: the bulk solvent, protein, and water bound to the protein. The relative importance of each component is determined by the time scale on which one is considering the quantum dynamics of the chromophore. Our results provide a natural explanation and model for the different time scales observed in the spectral density extracted from the solvation dynamics probed by ultra-fast laser spectroscopy techniques such as the dynamic Stokes shift and three pulse photon echo spectroscopy. Our results can be used to define under what conditions the dynamics of the chromophore is dominated by the surrounding protein and when it is dominated by dielectric fluctuations in the solvent.

Introduction

The functionality of many proteins is associated with a small subsystem or active site such as a heme group, a couple of amino acids involved in proton transfer, or a co-factor such as an optically active molecule (chromophore). There are a diverse range of optically active molecules that have an important biological function [1]. Examples include retinal (involved in vision), green fluorescent protein and porphyrins (photosynthesis). For these chromophores, the protein acts as a transducer which converts optical excitation of the chromophore into a change such as an electrical signal or conformational change that in turn brings about the desired biological function. Many of these transducers operate with speeds, specificities, and efficiencies which nanotechnologists are striving to mimic [2].

The dynamics of the protein involves thousands of degrees of freedom and at room temperature can be described by classical mechanics and modelled using molecular dynamics methods. In contrast, the functional subsystem involves only a few quantum states and their dynamics must be described quantum mechanically. This has led to considerable effort at developing hybrid QM/MM (quantum mechanical-molecular mechanical) methods [3]. In most cases the change in quantum state associated with the functional event is associated with a change in the electric dipole moment of the

*To whom correspondence should be addressed. E-mail: mckenzie@physics.uq.edu.au

subsystem. Since the protein contains polar residues and is surrounded by a highly polar solvent (water) [4, 5, 6, 7, 8] there is a strong interaction between the functional subsystem and its environment. Consequently, the environment can have a significant effect on the quantum dynamics of the subsystem.

This interplay between quantum and classical dynamics raises a number of questions of fundamental interest. On what length and time scales does the crossover from quantum to classical behaviour occur? When are quantum mechanical effects such as coherence (i.e., superposition states), entanglement, tunneling, or interference necessary for biological function? [9] What aspects and details of the structure and dynamic properties of the protein are crucial to biological function? Indeed chromophores such as retinal exhibit distinctly different dynamics in solution, in the gas phase, and in the protein environment [10].

1.1 Biomolecular chromophores

Most chromophores are large conjugated organic molecules which are surrounded by the protein which in turn is surrounded by a solvent. Figure 1 shows the photoactive yellow protein (PYP), including the chromophore and the so-called “bound water” molecules which reside with comparatively long lifetimes on the surface of the protein [11]. Most chromophores have large dipole moments which change significantly upon optical excitation, leading to significant relaxation of the polarisable environment. These systems exhibit a broad range of time, length and energy scales (see Figure 2). Typical values of different time scales are shown in Table 1.

In this paper, we specifically consider chromophores which can be described as two level systems (TLS) where a single excited state dominates (possibly from rapid internal conversion). This is often the HOMO (Highest Occupied Molecular Orbital) to LUMO (Lowest Unoccupied Molecular Orbital) transition. Such a model is particularly applicable to strongly fluorescent proteins, although in some cases excited state dynamics should still be considered (e.g., Green Fluorescent Protein [12]). The minimal models proposed here can also be extended to include internal dynamics, such as conformational change [5].

Questions of quantum coherence and the role of the environment are particularly pertinent and controversial in photosynthetic systems [13, 14, 15]. It has sometimes been claimed that the excitons within the light harvesting rings are quantum mechanically coherent over some or all of the chromophores (sometimes as many as 32) within the ring. It has also been suggested that such coherence is important for optimum performance of the system [16, 17, 18]. On the other hand, inter-ring transfer of excitons is incoherent which ensures the desirable feature of irreversible transport of energy towards the reaction centre.

1.2 Quantum dynamics, decoherence, and the spin-boson model

Understanding the quantum dynamics of a quantum system which is strongly coupled to its environment is a challenging theoretical problem that has attracted considerable attention over the past few decades [31, 32]. Substantial progress has been made by considering the simplest possible models such as the spin boson model [33] which describes a two-level system (the “spin”) which is coupled linearly to an infinite “bath” of harmonic oscillators,

$$H = H_0 + H_2 \quad (1)$$

where

$$H_0 = \sum_{\beta} \left(\frac{p_{\beta}^2}{2m_{\beta}} + \frac{1}{2}m_{\beta}\omega_{\beta}^2q_{\beta}^2 \right) \quad (2)$$

and

$$H_2 = \begin{pmatrix} \frac{\epsilon}{2} + \sum_{\beta} c_{\beta} \sqrt{\frac{2m_{\beta}\omega_{\beta}}{\hbar}}q_{\beta} & \Delta \\ \Delta & -\frac{\epsilon}{2} - \sum_{\beta} c_{\beta} \sqrt{\frac{2m_{\beta}\omega_{\beta}}{\hbar}}q_{\beta} \end{pmatrix} \quad (3)$$

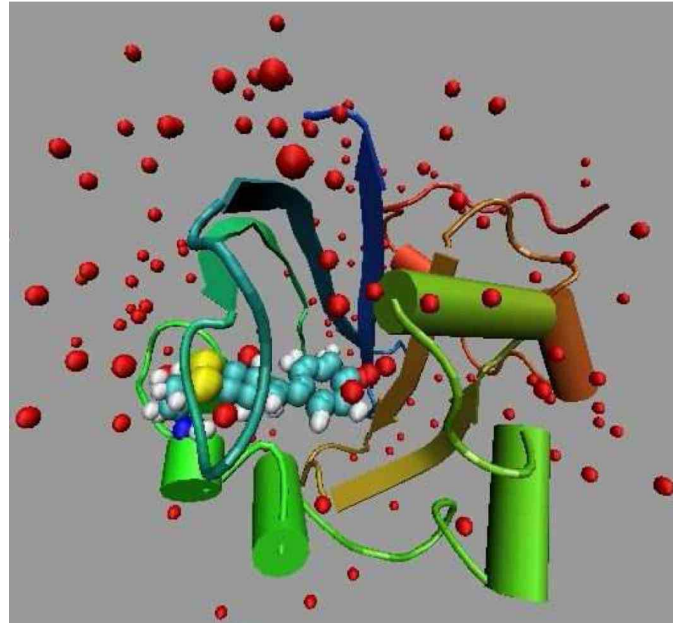


Figure 1: The chromophore, protein and bound water in photoactive yellow protein (PYP). The isolated spheres represent the bound water, the chromophore is shown by its van de Waals surface, and the protein by a cartoon representation. Observe that the chromophore is almost completely contained within the protein, shielded from direct contact with the surrounding bulk water. Generated from the Protein Database 3PYP.pdb[19].

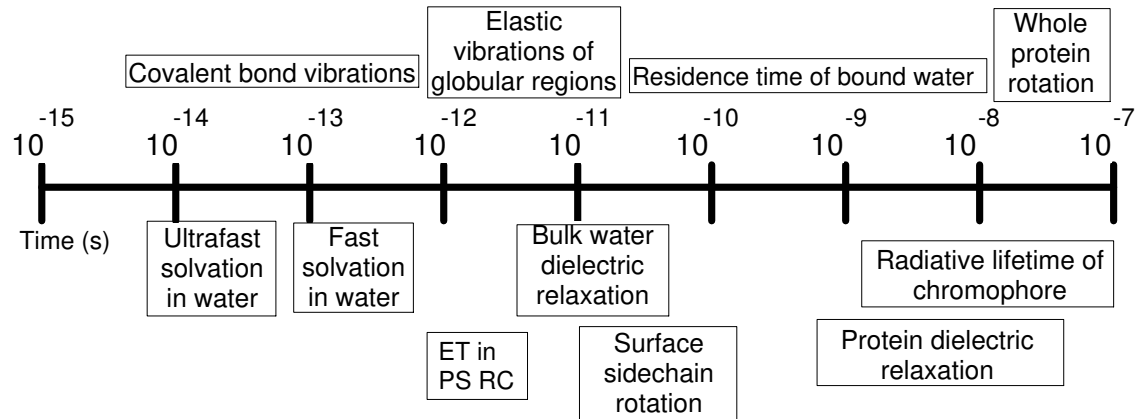


Figure 2: Schematic representation of the time scales of various processes in proteins and solutions. ET stands for electron transfer, PS RC for photosynthetic reaction centre. See Table 1 for specific numbers.

Table 1: Timescales for various processes in biomolecules and solutions. The radiative lifetime of a chromophore is order of magnitudes longer than all other timescales, except perhaps protein dielectric relaxation. MD refers to results from molecular dynamics simulations. Of particular relevance to this work is the separation of timescales, $\tau_s \ll \tau_b \ll \tau_p$ (compare Fig. 2).

Process	Timescale	Ref.
Radiative lifetime	10 ns	[20]
Internal conversion	10fs	[20]
Bulk water dielectric relaxation	8 ps	[21]
Protein dielectric relaxation (MD), $\tau_{D,p}$	1-10 ns	[22, 23]
Ultrafast solvation in water	10's fs	[24]
Fast solvation in water, τ_s	100's fs	[24]
Solvation due to bound water, τ_b	5-50 ps	[25]
Solvation due to protein, τ_p	1-10 ns	[26]
Covalent bond vibrations	10-100 fs	[20]
Elastic vibrations of globular regions	1-10 ps	[20]
Rotation of surface sidechains	10-100 ps	[20]
Reorientation of whole protein	4-15 ns	[23]

Table 2: Comparison of the matrix element Δ which couples two quantum states for various processes in proteins with the solvation rates due to the interaction of the quantum system with different parts of its environment. The quantum dynamics of the process will be determined largely by the part of the environment which undergoes solvation relaxation at a rate comparable to Δ . LHI and LHII refer to light harvesting complexes I and II in photosynthetic purple bacteria.

Process	Δ energy (meV)	Ref.
Förster coupling between chromophores in FRET spectroscopy	0.2-2	
Interring Förster coupling between chromophores in LHI and LHII	0.3	[16]
Intraring Förster coupling between two chlorophyl molecules in LHI	50-100	[16]
Electron transfer in photosynthetic reaction centre	1-10	[27]
Electron transfer in proteins	$10^{-4} - 10^{-2}$	[28]
Proton transfer	0.05	[29]
Level crossing for non-radiative decay	40	[30]
Solvation rate due to bulk water	8	[24]
Solvation rate due to bound water	0.1-1	[25]
Solvation rate due to protein	0.004-0.04	[26]

In terms of second quantised operators a_β, a_β^\dagger this can be written

$$H = \frac{1}{2}\epsilon\sigma_z + \Delta\sigma_x + \sum_\beta \hbar\omega_\beta a_\beta^\dagger a_\beta + \sigma_z \sum_\beta C_\beta (a_\beta^\dagger + a_\beta), \quad (4)$$

where σ_x and σ_z are Pauli spin matrices, the C_β describes the coupling of the system to each bath mode β , ϵ is the separation of system energy levels and Δ is the tunneling matrix element coupling the two states. Another model is the spin-bath model [34], where the system of interest is coupled to specific localised states of the environment, themselves treated as two level systems.

For the spin-boson model, the quantum dynamics is completely determined by a single function, the spectral density, which is defined by

$$J(\omega) = \frac{4\pi}{\hbar} \sum_\beta C_\beta^2 \delta(\omega - \omega_\beta). \quad (5)$$

It describes how strongly the oscillators with frequency near ω are coupled to the two-level system. Many systems are described by ohmic dissipation, for which $J(\omega) = \hbar\omega$ below some cutoff frequency, ω_c , related to the relaxation rate of the environment, and above which the coupling to the bath of oscillators can be neglected. The main purpose of this paper is to derive physically realistic expressions for this spectral density that are relevant to biological chromophores interacting with their environment.

If $\epsilon, \Delta \ll \hbar\omega_c$, for ohmic dissipation α is a critical parameter for determining the qualitative properties of the quantum dynamics [33, 31, 35]. At zero temperature, for $\alpha < \frac{1}{2}$ the state of the TLS, exhibits damped Rabi oscillations, a signature of quantum coherence and interference. This can be described by considering the time dependence of the probability that the system is in one of the two levels, which can be related to the expectation value $\langle \sigma_z(t) \rangle$. For $\frac{1}{2} < \alpha < 1$, the system exhibits incoherent relaxation (exponential decay of $\langle \sigma_z(t) \rangle$), and for $\alpha > 1$ the system is localised in its initial state - an example of the quantum Zeno effect [36]. A non-zero temperature reduces the range of α over which coherent oscillations can occur (see Fig. 21.2 in [31]).

If $\Delta > \hbar\omega_c$ then the results of Refs. [33] and [35] do not apply [37]. The bath responds slower than the TLS. Consequently, in order to destroy coherent oscillations, the bath must couple more strongly to the two-level system than for the case $\Delta \ll \hbar\omega_c$. System dynamics has been studied with quantum Monte Carlo simulations [38]. Coherent oscillations in $\langle \sigma_z(t) \rangle$ may be present for $\alpha > 1$, e.g., from Fig. 13 in Ref. [38] if $\Delta = 6\hbar\omega_c$ then coherent oscillations can exist even for $\alpha = 30$. Fig. 8 of Ref. [39] shows that for $\Delta = \hbar\omega_c$, coherent oscillations exist for $\alpha < 1.5$.

The quantum dynamics of the spin boson model (4) for a general spectral density $J(\omega)$ will be largely determined by the magnitude and frequency dependence of $J(\omega)$ for $\omega \sim \Delta$. For example, when the bath is weakly coupled to an unbiased ($\epsilon = 0$) two level system (i.e., $J(\Delta) \ll \Delta$) coherent oscillations exist, and the relevant decoherence rate given [33] by Fermi's Golden Rule is

$$\frac{1}{T_2} = J(\Delta) \coth \left(\frac{\Delta}{2k_B T} \right). \quad (6)$$

Knowledge of the spectral density $J(\omega)$ allows one to make definite statements about whether the quantum dynamics is coherent. For biomolecular systems, the spin-boson model has previously been applied to electron transfer [40, 3] and proton transfer [41]. We have recently shown its relevance to understanding the effect of the environment on Förster resonant energy transfer between two chromophores[4].

Of particular interest is when two molecules are coupled by Resonance Energy Transfer (RET), such as rings of chlorophyll molecules in photosynthesis and in Fluorescent Resonance Energy Transfer spectroscopy (FRET). Here, an excitation in one chromophore may be transferred to a nearby chromophore by the Coulomb interaction, typically dipole-dipole interactions. A coupled system of molecules such as this may be mapped to the spin-boson model [5], where the two quantum states refer to the location of the excitation, ϵ is the difference in the two chromophore's excited

energy levels, and $J(\omega)$ describes the coupling of the excitation to the environments surrounding each molecule. We have previously shown [5] that the appropriate spectral density is simply the sum of the spectral density of each individual chromophore-protein complex. The magnitude of the spectral density then determines whether the transfer is coherent (oscillatory) or incoherent (one-way). There are several definite experimental signatures of the coherent interaction of a pair of chromophores. These include (Davydov) splitting of energy levels [20], super- and sub-radiance (i.e., increase and reduction of the radiative life time [42, 18]) and changes in fluorescence anisotropy [43]. Both coherence (within a ring) and incoherence (between rings) may play potentially important functional roles in light harvesting complexes.

1.3 The chromophore environment: protein, bound water, and bulk water

The structures and dynamics associated with the interaction of proteins with water is extremely rich and a challenge to model and to understand.[6, 7, 8, 44]. One can classify the water molecules associated with proteins into several categories. (i) Water which is distant from the protein and has the same properties as bulk water. (ii) Water at the surface of the protein molecule. The first layer of molecules is referred to as the first hydration or solvation layer. These molecules are weakly bound to the charged residues found at the protein surface. (iii) Water buried inside the protein and which often binds to specific sites in the protein via multiple hydrogen bonds. The water inside and at the surface of the protein can exchange with the bulk water.

Advances in experimental probes such as neutron scattering [44], nuclear magnetic resonance (NMR)[8], femtosecond laser spectroscopy,[45] and dielectric dispersion [46] has allowed a quantitative description of the properties of the water molecules associated with specific parts of the solvated protein. Key quantities that can be determined include, (a) the occupancy (i.e., the probability that a water molecule will be found at the site), (b) the residence time (the timescale for exchange of the water molecule with the surrounding bulk water), and (c) the “order parameter” which is a measure of the rotational freedom of the water molecule at the site. NMR measurements suggest that the molecules at the surface exchange with the bulk water on timescales ranging from 10 psec to 1 nsec[8]. In contrast, buried molecules exchange with the solvent on timescales of the order of 1 ns to 1 μ s [7, 8].

The term “biological water” has been used to describe water in proximity to a biological macromolecule [47]. Dielectric relaxation is significantly different in biological water [48]. Whereas in bulk water the dominant dielectric relaxation time is 8.3 ps, for bound water this can be 2 to 4 orders of magnitude larger. Dielectric spectroscopy measurements of proteins in aqueous solutions found four dielectric relaxation times.[46] For myoglobin these times were attributed to (1) reorientation of bulk water (8 ps), (2) relaxation of water associated with the protein (10 ps and 150 ps), and (3) reorientation of the whole protein molecule (15 nsec).

1.4 Overview of the paper

In this paper we consider five distinct dielectric continuum models of the environment of a biological chromophore. For each model we derive an expression for the spectral density (5). This allows us to explore how the relative importance of the dielectric relaxation of the solvent, bound water, and protein depends on the relevant length scales (the relative size of the chromophore, the protein and the thickness of the layer of bound water) and time scales (the dielectric relaxation times of the protein, bound water and the solvent) as is discussed in Section 5. Many experimentally obtained spectral densities can be fitted to a sum of Lorentzians of the form

$$J(\omega) = \frac{\alpha_1 \omega}{1 + (\omega \tau_1)^2} + \frac{\alpha_2 \omega}{1 + (\omega \tau_2)^2} + \dots \quad (7)$$

For a protein that is large compared to the size of the binding pocket of the chromophore and the width of the bound water layer, our models predict a spectral density given by the sum of three Lorentzians which correspond to the dynamics of the protein, bound water and bulk water dynamics respectively. This is shown schematically in Figure 3.

Key to this is the separation of time scales, associated with the solvation coming from each of the three components of the environment.

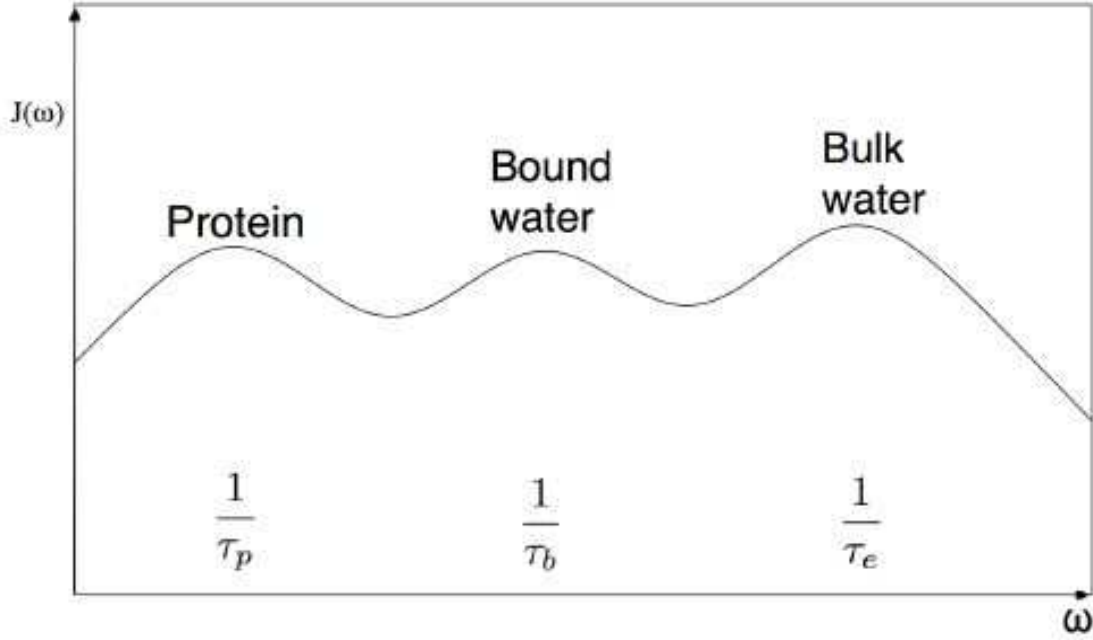


Figure 3: Schematic plot of the spectral density for a typical chromophore on a log-log scale. We see three distinct peaks, which can be attributed to the relaxation of the protein, bound water and bulk solvent, respectively

Specifically, to a good approximation, the spectral density is given by,

$$J(\omega) = \frac{\alpha_p \omega}{1 + (\omega \tau_p)^2} + \frac{\alpha_b \omega}{1 + (\omega \tau_b)^2} + \frac{\alpha_s \omega}{1 + (\omega \tau_s)^2} \quad (8)$$

where the relaxation times can be expressed as:

$$\frac{\tau_p}{\tau_{D,p}} = \frac{2\epsilon_{p,i} + 1}{2\epsilon_{p,s} + 1} \quad (9)$$

$$\frac{\tau_s}{\tau_{D,s}} = \frac{2\epsilon_{s,i} + 1}{2\epsilon_{s,s} + 1} \quad (10)$$

$$\tau_b = \tau_{D,b} \quad (11)$$

The subscripts $x = p, s, b$ refer to the protein, solvent and bound water respectively, and $\epsilon_{x,s}, \epsilon_{x,i}, \tau_{D,x}$ are the static dielectric constant, high frequency dielectric constant, and relaxation times of a Debye model for each medium $x = p, e, b$.

The reorganisation energies associated with each part of the environment are given by α_i/τ_i , where

$$\frac{\alpha_p}{\tau_p} = \frac{(\Delta\mu)^2}{2\pi\epsilon_0 a^3} \frac{6(\epsilon_{e,s} - \epsilon_{e,i})}{(2\epsilon_s + 1)(2\epsilon_{e,i} + 1)} \quad (12)$$

$$\frac{\alpha_s}{\tau_s} = \frac{(\Delta\mu)^2}{2\pi\epsilon_0 b^3} \frac{6(\epsilon_{e,s} - \epsilon_{e,i})}{(2\epsilon_s + 1)(2\epsilon_{e,i} + 1)} \left(\frac{9\epsilon_{p,i}}{(2\epsilon_{p,i} + 1)^2} \right) \quad (13)$$

$$\frac{\alpha_b}{\tau_b} = \frac{3(\Delta\mu)^2}{2\pi\epsilon_0 b^3} \left(\frac{c - b}{b} \right) \frac{(\epsilon_{b,s}^2 + 2\epsilon_{e,s}^2)(\epsilon_{b,s} - \epsilon_{b,i})}{\epsilon_{b,s}^2(2\epsilon_{e,s} + 1)^2} \quad (14)$$

In particular, for typical systems the above three quantities can be of the same order of magnitude, i.e.,

$$\frac{\alpha_s}{\tau_s} \sim \frac{\alpha_b}{\tau_b} \sim \frac{\alpha_p}{\tau_p}. \quad (15)$$

Hence, the peaks of the spectral density can be of the same order of magnitude. This is because although each contribution is due to different dielectrics constants, they only have a limited range of values. This is supported by experimental data (see Table 3) where several relaxation times are observed which vary by several orders of magnitude, but whose relative contributions are comparable. Therefore, in many cases only a single component of the environment (protein, bound water, bulk solvent) will be relevant to a given process. These expressions allow us to predict the ultrafast solvation times in the presence of a protein, which we find may increase the solvation time by at most a factor of two. We also suggest that at least some of studies which have identified ultrafast dielectric relaxation of proteins [49, 50] may in fact be detecting the fast response of the distant solvent.

The outline of the paper is as follows. In Section 2 we describe how the interaction between a chromophore and its protein and solvent environment may be modelled by an independent boson model. In Section 3 we propose a set of continuum dielectric models suitable for describing the environment around a chromophore, and use them to obtain an expression for the spectral density in each case. In Section 4 we consider particular limits of these spectral densities and obtain simple expressions for the contribution of each component of the environment (protein, bound water, and bulk water) to the total spectral density. In particular, we are able to obtain expressions that can be used to evaluate the relative importance of each component of the environment. We find that even when the chromophore is completely surrounded by a protein it is possible that the ultra-fast solvation (on the psec timescale) is dominated by the bulk solvent surrounding the protein. In Section 5 we discuss methods for obtaining spectral densities from optical spectroscopy, and compare the predictions of our models to experimental data. In Section 6 we relate our results for the spectral density and dielectric relaxation to what has been learnt from molecular dynamics simulations on specific protein systems.

2 Independent boson model for chromophore-environment interaction

It can be shown [5] that the coupling of the electronic excitations in a chromophore to its environment may be modelled by an independent boson model [51] of the form

$$H = \frac{1}{2}\epsilon\sigma_z + \sum_{\beta} \omega_{\beta} a_{\beta}^{\dagger} a_{\beta} + \sigma_z \sum_{\beta} C_{\beta} (a_{\beta} + a_{\beta}^{\dagger}). \quad (16)$$

Here the chromophore is treated as a two level system with energy gap ϵ between the ground and excited state. The first term describes the energy of the isolated chromophore, described by Pauli sigma matrix σ_z . The second term

is the energy of the surrounding environment (protein and solvent), where the environment is modelled as a bath of harmonic oscillators [5]. The final term describes the coupling of the state of the chromophore σ_z to the environment. In this case, the coupling [52, 53] is due to electrostatic interactions between the chromophore dipole and the “cage” of polarised solvent and protein molecules around it, as will be described in more detail below. The effect of this coupling on the quantum dynamics of the chromophore is completely specified by the spectral density, defined by eq. (5) [51]. For example, if the two-level system is initially in a state specified by a 2×2 density matrix, $\rho(0)$, then at time t , the density matrix has matrix elements [54]

$$\begin{aligned}\rho_{11}(t) &= \rho_{11}(0) \\ \rho_{22}(t) &= \rho_{22}(0) = 1 - \rho_{11}(0) \\ \rho_{12}(t) &= \rho_{21}^*(t) = \rho_{12}(0) \exp(-i\epsilon t + i\theta(t) - \Gamma(t, T))\end{aligned}\quad (17)$$

where $\theta(t)$ is a phase shift given by

$$\theta(t) = \int_0^\infty J(\omega) \frac{[\omega t - \sin(\omega t)]}{\omega^2} d\omega \quad (18)$$

and

$$\Gamma(t, T) = \int_0^\infty d\omega J(\omega) \coth\left(\frac{\omega}{2k_B T}\right) \frac{(1 - \cos \omega t)}{\omega^2} \quad (19)$$

describes the decoherence due to interaction with the environment.

Depending on the relative size of the time t to the time scales defined by $1/\omega_c$ and $\hbar/k_B T$, there are three different regimes of time dependence. For short times $\omega_c t < 1$,

$$\Gamma(t, T) = \frac{t^2}{2\tau_g^2} \quad (20)$$

where

$$\frac{1}{\tau_g^2} = \int_0^\infty d\omega J(\omega) \coth\left(\frac{\omega}{2k_B T}\right) \quad (21)$$

and so there is a Gaussian decay of decoherence. For $k_B T \gg \hbar\omega_c$, this reduces to

$$\frac{\hbar}{\tau_g} = \sqrt{2E_R k_B T} / \hbar \quad (22)$$

where E_R is the reorganisation energy given by

$$E_R = \int_0^\infty \frac{J(\omega)}{\omega} \quad (23)$$

If $J(\omega) = \frac{\alpha\omega}{1+(\omega/\omega_c)^2}$ then for intermediate times (the quantum regime [55]),

$$\Gamma(t, T) \approx \alpha \ln(\omega_c t) \quad (24)$$

and for long times ($t \gg \hbar/k_B T$, the thermal regime)

$$\Gamma(t, T) \approx 2\alpha k_B T t / \hbar. \quad (25)$$

3 The spectral density for the different continuum models of the environment

3.1 Different models

In the simplest (continuum model [56]) picture of protein-pigment complexes, the chromophore can be treated as a point dipole inside a spherical dielectric [56, 53], representing the protein, surrounded by a uniform polar solvent with complex dielectric constant $\epsilon_e(\omega)$ [52]. This can also apply to a chromophore-protein complex embedded in a solid dielectric medium. In a previous work [5], the spectral density was determined for a free chromophore in a solvent. However, most chromophores are inside proteins, which may have a significant effect, if only in pushing back the solvent.

Several continuum dielectric models for the protein environment have previously been proposed (see for example Figure 2 in ref. [56] and Figure 2 in ref. [57].) We consider five distinct models, illustrated in figure 4. Model 1 describes a free chromophore with no surrounding protein. The molecule sits inside a spherical cavity of radius a , approximately the van de Waals radius of the molecule, inside a solvent with dielectric constant $\epsilon_e(\omega)$. Model 2 describes an analogous situation, but this time the chromophore is surrounded by an infinite, uniform protein with complex dielectric constant $\epsilon_p(\omega)$ again inside a cavity of radius a , which would typically be approximately the same radius as for Model 1. In Model 3 the chromophore is surrounded by a uniform dielectric sphere representing the protein. This sphere has radius b and dielectric constant ϵ_p . In a more detailed picture, Model 4 (see Figure 5, the Models 2 and 3 are combined so that the chromophore sits inside a hollow cavity within the protein. The cavity has radius a and vacuum dielectric constant ϵ_0 , while the protein again has radius b and is now described by complex dielectric constant $\epsilon_p(\omega)$. Further detail may be added by treating the outer layer of the protein sphere as a separate, higher dielectric medium [56] representing the charged surface groups [58]. In all cases, the chromophore is treated as a point dipole. In Model 5, the chromophore sits in a static protein (no cavity) and is surrounded by a thin shell of bound water with a different dielectric constant to the bulk solvent.

In every case, the central chromophore dipole polarises the surrounding cage of protein and solvent, which in turn produces an electric field inside the cavity, called the *reaction field*. The interaction of this field with the central dipole is responsible for the interaction between the chromophore and its environment. The independent boson model can be obtained by writing the reaction field in terms of its normal modes, and quantising the coefficients in the standard second quantisation method.

3.2 Solution for the reaction field

The reaction field for these models can be obtained by a generalisation of the techniques in ref. [53], as follows: The electric potential, $\phi(x, y, z)$, satisfies Poisson's equation $\nabla^2\phi = -\rho/\epsilon$, where ϵ is the local dielectric constant of the medium and ρ is the local charge density. Away from the point dipole and surface boundaries, $\rho = 0$ and we must solve Laplace's equation $\nabla^2\phi = 0$. At the dielectric boundaries (and in general), ϕ must be continuous and because there are no free charges, $\vec{D} = \epsilon\vec{E} = -\epsilon\nabla\phi$ is also continuous across the boundaries.

Although the protein is spherically symmetric, because of the point-dipole, the system has only cylindrical symmetry. If the spherically symmetric electric potential in each concentric dielectric shell is given by $\phi_1(r), \phi_2(r), \dots$, we can expand ϕ_i in terms of spherical harmonics [53]:

$$\phi_i = \sum_{n=0}^{\infty} \left(A_{i,n} r^n + \frac{B_{i,n}}{r^{n+1}} \right) P_n(\cos\theta)$$

We consider explicitly the case where we have a cavity surrounded by a single dielectric shell inside a bulk solvent. The central cavity has radius a , dielectric ϵ_c and potential $\phi_c(r, \omega)$, the shell has total radius b (thickness $b - a$), dielectric

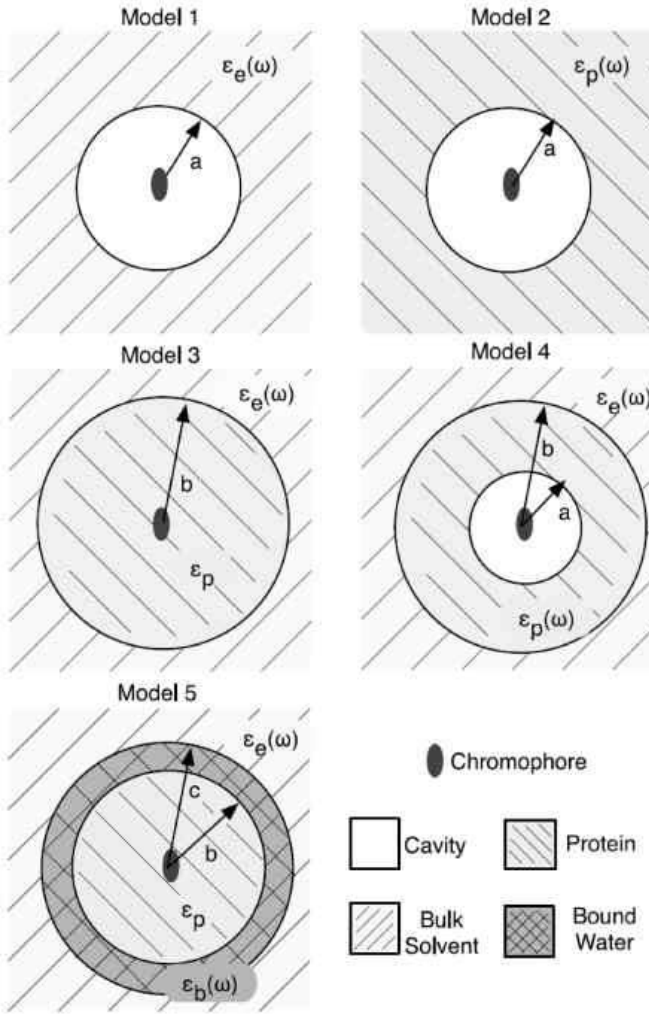


Figure 4: The five models considered for a chromophore-protein-solvent system. The chromophore is modelled as a point dipole. In Model 1, the chromophore is modelled sits at the centre of a cavity of radius a roughly of the Van de Waals size of the chromophore, surrounded by a uniform polar solvent with complex dielectric constant $\epsilon_e(\omega)$. In Model 2, the chromophore is surrounded by an infinite protein, modelled as a uniform, continuous dielectric medium, with complex dielectric constant $\epsilon_p(\omega)$. In Model 3, the chromophore sits in a protein of radius b surrounded by the solvent. In Model 4, the chromophore sits in a cavity inside the dynamic protein, surrounded by solvent. In Model 5, the static protein is surrounded by a thin shell of bound water of radius c , surrounded by the bulk solvent.

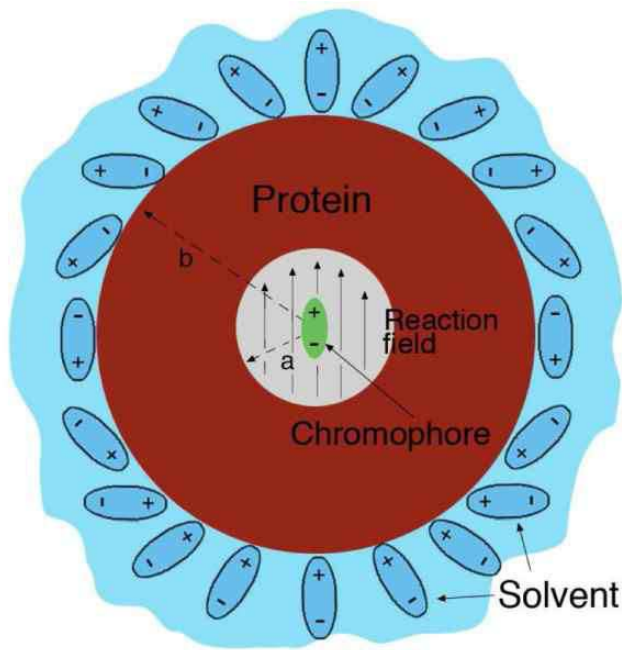


Figure 5: Model 4 for the interaction between a chromophore and its environment. The chromophore is treated as a point dipole sitting in a cavity of radius a in the centre of a spherical, uniform protein which is treated as a homogeneous dielectric medium of radius b . The protein-pigment complex is surrounded by a solvent, typically water, which is again treated as a homogeneous dielectric medium though actual molecules are shown for clarity of explanation. The chromophore's dipole moment polarises its environment, which in turn produces an electric field, the "reaction field", which interacts with the chromophore. Fluctuations in the environment will translate to fluctuations in the chromophore's energy.

ϵ_p and potential $\phi_p(r, \theta)$, and the bulk environment is described by dielectric ϵ_e and potential $\phi_e(r, \omega)$.

We can then apply the boundary conditions:

$$\phi_e(r \rightarrow \infty) \rightarrow 0 \quad (26a)$$

$$\phi_\mu = \frac{\mu}{r^2} \cos \theta \quad (26b)$$

$$(\phi_p)_{r=b} = (\phi_e)_{r=b} \quad (26c)$$

$$(\phi_c)_{r=a} = (\phi_p)_{r=a} \quad (26d)$$

$$\epsilon_c \left(\frac{\partial \phi_c}{\partial r} \right)_{r=a} = \epsilon_p \left(\frac{\partial \phi_p}{\partial r} \right)_{r=a} \quad (26e)$$

$$\epsilon_p \left(\frac{\partial \phi_p}{\partial r} \right)_{r=b} = \epsilon_e \left(\frac{\partial \phi_e}{\partial r} \right)_{r=b} \quad (26f)$$

The first condition is that the potential must go to zero at infinity. This means that all coefficients with positive powers of r must vanish, i.e., $A_{e,n} = 0$ for all n .

The second condition is the field from a point dipole. As this is the only free charge in the cavity, this is the only source term (inverse power of r) that will contribute to the potential $\phi(r, \theta)$. Since $P_1(\cos \theta) = \cos \theta$, only the $n = 1$ term is involved. Therefore, $B_{c,n=1} = \mu$ and $B_{c,n \neq 1} = 0$. (Nothing is said about $A_{c,n}$).

The final terms describe the continuity of the potential and its derivative over the boundary. The first condition gives

$$\sum_{n=0}^{\infty} \left(A_{p,n} b^n + \frac{B_{p,n}}{b^{n+1}} \right) P_n(\cos \theta) = \sum_{n=0}^{\infty} \frac{B_{e,n}}{b^{n+1}} P_n(\cos \theta) \quad (27)$$

Because the spherical harmonics P_n are orthogonal, we can consider each term of this sum as being equal, so

$$A_{p,n} b^n + \frac{B_{p,n}}{b^{n+1}} = \frac{B_{e,n}}{b^{n+1}} \quad (28)$$

In a similar way, the remaining boundary conditions can be applied to produce a set of linear equations on the $A_{i,n}$ and $B_{i,n}$. We have six boundary conditions and six variables (each, of course, a function of n) and so we are able to solve for all parameters. However, we are only interested in the field inside the cavity, and in particular the unknown part $A_{c,n}$. We find that all the $A_{c,n}$ are zero except for $n = 1$. Thus, the potential due to the surface charges is given by $\phi_{c,\text{surf}} = -\chi \mu r \cos \theta = -\chi \mu \hat{z}$ where we find

$$\chi(\omega) = \frac{2}{a^3} \frac{(\epsilon_p + 2\epsilon_c)(\epsilon_e - \epsilon_p)a^3 + (\epsilon_p - \epsilon_c)(2\epsilon_e + \epsilon_p)b^3}{2(\epsilon_p - \epsilon_c)(\epsilon_e - \epsilon_p)a^3 + (2\epsilon_p + \epsilon_c)(2\epsilon_e + \epsilon_p)b^3} \quad (29)$$

The actual electric field in the cavity due to the surface charges but not the dipole itself – the reaction field – is then $\vec{R} = R\hat{z} = -\nabla \phi_{e,\text{surf}}(x, y, z) = \chi \mu \hat{z}$, which will be a constant throughout the cavity, parallel to the dipole, and proportional to the dipole moment μ . The spectral density describing coupling of changes in the chromophore state to this environment is related to the zero temperature fluctuations in the reaction field [5]:

$$J(\omega) = (\Delta\mu)^2 \text{Re} \int dt e^{i\omega t} \langle R(t)R(0) \rangle_{T=0} \quad (30)$$

This can be shown by writing the reaction field $R(t)$ in terms of its normal modes' creation and annihilation operators. $\Delta\mu$ is the change in chromophore dipole moment on the transition from the ground to excited states. The fluctuations

in the reaction field $\langle R(t)R(0) \rangle$ are obtained [5] from the fluctuation dissipation theorem, and are proportional to the imaginary part of $\chi(\omega)$ in (29) above, yielding

$$J(\omega) = 2(\Delta\mu)^2 \text{Im}(\chi(\omega)) \quad (31)$$

Note the use of zero temperature fluctuations is a mathematical derivation only, and provided the appropriate temperature parameters for the solvent and protein are used, the resulting spectral density is applicable to all temperatures.

3.3 Spectral densities of different Models

For Model 1, with no protein, the spectral density is

$$J_e(\omega) = \frac{(\Delta\mu)^2}{4\pi\epsilon_0 a^3} \text{Im} \frac{2(\epsilon_e(\omega) - \epsilon_c)}{2\epsilon_e(\omega) + \epsilon_c}. \quad (32)$$

where a is the radius of the cavity containing the chromophore and $\epsilon_e(\omega)$ is the complex dielectric function of the solvent and ϵ_c the (static) dielectric constant of the cavity. $\Delta\mu$ is the change in dipole moment of the chromophore during the transition.

For Model 2, with no solvent, the spectral density has the identical form to Model 1, except we use the dielectric constant of the protein $\epsilon_p(\omega)$:

$$J_p(\omega) = \frac{(\Delta\mu)^2}{4\pi\epsilon_0 b^3} \text{Im} \frac{2(\epsilon_p(\omega) - \epsilon_c)}{2\epsilon_p(\omega) + \epsilon_c}. \quad (33)$$

where b is the radius of the protein containing the chromophore, $\epsilon(\omega)$ is the complex dielectric function of the solvent and $\epsilon_p(\omega)$ is the complex dielectric function of the protein.

For Model 3, both the protein and the solvent are included, and the spectral density is

$$J_{pe}(\omega) = \frac{(\Delta\mu)^2}{4\pi\epsilon_0 b^3} \text{Im} \frac{2(\epsilon_e(\omega) - \epsilon_p)}{2\epsilon_e(\omega) + \epsilon_p}. \quad (34)$$

where b is the radius of the protein containing the chromophore, $\epsilon(\omega)$ is the complex dielectric function of the solvent and ϵ_p is an appropriate (constant) dielectric function of the protein.

For Model 4, where the chromophore sits in a cavity in the centre of the protein which is in turn surrounded by the solvent, we will refer to the spectral density as the "full" spectral density. It is given by:

$$J_{\text{full}}(\omega) = \frac{(\Delta\mu)^2}{2\pi\epsilon_0 a^3} \text{Im} \frac{(\epsilon_p + 2)(\epsilon_e - \epsilon_p)a^3 + (\epsilon_p - 1)(2\epsilon_e + \epsilon_p)b^3}{2(\epsilon_p - 1)(\epsilon_e - \epsilon_p)a^3 + (2\epsilon_p + 1)(2\epsilon_e + \epsilon_p)b^3} \quad (35)$$

where b is the radius of the protein containing the chromophore, a is the radius of the cavity containing the chromophore (usually the size of the chromophore), ϵ_e is the complex dielectric function of the solvent and ϵ_p is now the complex dielectric function of the protein. Note that the frequency dependence of the dielectric constants has been omitted for clarity. We see that for appropriate limits ($(a/b) \rightarrow 0$, $\epsilon_p = \epsilon_e$, $\epsilon_p = 1$, etc) Models 1 and 2 can be recovered, as expected. (To obtain Model 3, one would have to allow the centre cavity to have an arbitrary dielectric constant.)

For Model 5, we simply use the results of Model 4, where $\epsilon_p \rightarrow \epsilon_b$, $\epsilon_c \rightarrow \epsilon_p$, $a \rightarrow b$, $b \rightarrow c$:

$$J_{\text{bound}}(\omega) = \frac{(\Delta\mu)^2}{2\pi\epsilon_0 b^3} \text{Im} \frac{(\epsilon_b + 2\epsilon_p)(\epsilon_e - \epsilon_b)b^3 + (\epsilon_b - \epsilon_p)(2\epsilon_e + \epsilon_b)c^3}{2(\epsilon_b - \epsilon_p)(\epsilon_e - \epsilon_b)b^3 + (2\epsilon_b + \epsilon_p)(2\epsilon_e + \epsilon_b)c^3} \quad (36)$$

Note that ϵ_p refers to a constant (typically high frequency) protein dielectric viz. Model 2. ϵ_b is the complex dielectric of the bound water.

3.4 Frequency dependence of dielectric constants

To specify the dielectric constant of the solvent $\epsilon_e(\omega)$ we consider the Debye form of the dielectric [59],

$$\epsilon_e(\omega) = \epsilon_{e,i} + \frac{\epsilon_{e,s} - \epsilon_{e,i}}{1 - i\omega\tau_D} \quad (37)$$

where τ_D is the Debye relaxation time of the solvent, $\epsilon_{e,s} = \epsilon(\omega = 0)$ is the static dielectric constant and $\epsilon_{e,i} = \epsilon(\omega \rightarrow \infty)$ is the high frequency dielectric constant, within the range of physically relevant frequencies – note that $\epsilon_{e,i}$ would always be 1 for sufficiently high frequencies [60]. For water at room temperature, $\epsilon_s = 78.3$, $\epsilon_i = 4.21$ and $\tau_D = 8.2$ ps [21] while for THF (tetrahydrofuran) the values are $\epsilon_s = 8.08$, $\epsilon_i = 2.18$ and $\tau_D = 3$ ps [61].

In Model 4, the protein is treated as a complex frequency dependent dielectric with dielectric constant $\epsilon_p(\omega)$, and as such is allowed to relax and respond to the chromophore. We will consider the case of a Debye dielectric [60], but a more complicated model including multiple relaxation times is also possible [62]. Typical values for ϵ_p are between 4–40 depending on which part of the protein is of interest [63, 56, 22]. Studies also suggest that charged groups on the surface of the protein can skew the average value of the protein dielectric, and it may be more appropriate to model such proteins as having an inner and an outer shell with two different dielectric constants. The high frequency constant, which is the only value used by many studies, is more difficult to determine but is generally assumed to be between 1.5 and 2.5 [64, 18].

The appropriate dielectric relaxation time of the protein may be different from the protein relaxation times, which can be of order milliseconds [20], as there are processes (e.g., vibration of bonds) on the order of femtoseconds [20, p132, Table 3.13] which may contribute to the dielectric function. These may be missed in studies of the dielectric constant on the nanosecond timescale [65] and is perhaps unobservable for aqueous solutions of proteins (e.g., ref. [66]). Molecular dynamics simulations [22] suggest a protein dielectric relaxation time of 10 ns for a peptide, while vibrations may be of the order of 100 fs which may apply in certain situations. Other studies have found no simple relaxation times, with relaxation processes occurring across the entire experimental range of 20 ps – 20 ns [67]. For such proteins, alternatives to the Debye model may be more appropriate.

For Model 3, an appropriate value for the constant dielectric of the protein must be chosen, which will depend on the frequency range of physical interest. For example, for frequencies greater than $1/\tau_p$, where τ_p is approximately the protein dielectric relaxation time, the protein will be well approximated by its high frequency value.

The hydration shell of hydrogen bonded water molecules surrounding the protein may also have a dielectric constant different to that of the bulk solvent. In this case, an extra shell could be included around the protein with a longer Debye relaxation time. The spectral density for these models may be calculated through the same procedure described above, and while the complexity of the expression increases with the number of shells an exact expression for $J(\omega)$ may still be obtained by inserting the appropriate parameters.

4 Evaluation of the Ohmic coupling constant α for different models

We now attempt to determine an explicit form of the spectral density for each model, using Debye spectral densities, and where possible determine a dimensionless coupling constant for the strength of the interaction with each part of the environment.

For Ohmic spectral densities, we can define a dimensionless coupling parameter α such that at low frequencies (i.e., below the appropriate cut-off frequency $\omega_{c,i} \approx 1/\tau_i$) $J(\omega) = \alpha\omega$ which, with the cut-off frequencies defined above, gives all necessary information about the spectral density. This can be obtained by Taylor expanding the spectral density around $\omega = 0$. Even for non-Ohmic spectral densities, this coupling constant can still be defined for different components of the system if separate, Ohmic contributions from each sub-system can be identified. Another quantity

of particular physics interest is the reorganisation energy E_R , which is a measure of the energy required to polarise the environment upon a transition from the ground to excited states. It is given by eq. (23). Using the Drude form $J(\omega) = \alpha\omega/(1 + (\omega/\omega_c)^2)$ of the spectral density, we find

$$E_R = \pi\alpha\omega_c/2. \quad (38)$$

4.1 Model 1 - No protein

For the Debye form of the dielectric constants above,

$$J_e(\omega) = \frac{(\Delta\mu)^2}{2\pi\epsilon_0 a^3} \frac{6(\epsilon_{e,s} - \epsilon_{e,i})}{(2\epsilon_s + \epsilon_c)(2\epsilon_{e,i} + \epsilon_c)} \frac{\omega\tau_e}{\omega^2\tau_E^2 + \epsilon_c}, \quad (39)$$

where $\epsilon_{e,s}$ and $\epsilon_{e,i}$ are the static and high frequency frequency dielectric constants of the solvent respectively, and $\tau_e = \frac{2\epsilon_i + \epsilon_c}{2\epsilon_s + \epsilon_c}\tau_{D,e}$ where $\tau_{D,e}$ is the Debye relaxation time of the solvent. We note that the spectral density is Ohmic, with a cut-off frequency $\omega_c = 1/\tau_E$. If $\epsilon_c = 1, \epsilon_{e,i} = 1$ this is the usual Onsager model expression. The coupling constant is

$$\alpha_e = \frac{(\Delta\mu)^2}{2\pi\epsilon_0 a^3} \frac{6\tau_e(\epsilon_{e,s} - \epsilon_{e,i})}{(2\epsilon_s + \epsilon_c)(2\epsilon_{e,i} + \epsilon_c)} \quad (40)$$

4.2 Model 2 - No solvent

For Model 2, we get a similar result, but involving the protein dielectric constant:

$$J_p(\omega) = \frac{(\Delta\mu)^2}{2\pi\epsilon_0 a^3} \frac{6(\epsilon_{p,s} - \epsilon_{p,i})}{(2\epsilon_{p,s} + \epsilon_c)(2\epsilon_{p,i} + \epsilon_c)} \frac{\omega\tau_P}{\omega^2\tau_P^2 + 1}, \quad (41)$$

$$\alpha_p = \frac{(\Delta\mu)^2}{2\pi\epsilon_0 a^3} \frac{6\tau_p(\epsilon_{p,s} - \epsilon_{p,i})}{(2\epsilon_{p,s} + \epsilon_c)(2\epsilon_{p,i} + \epsilon_c)} \quad (42)$$

where $\epsilon_{p,s}$ and $\epsilon_{p,i}$ are the static and high frequency frequency dielectric constants of the protein respectively, and $\tau_p = \frac{2\epsilon_{p,i} + \epsilon_c}{2\epsilon_{p,s} + \epsilon_c}\tau_{D,p}$ where $\tau_{D,p}$ is the Debye relaxation time of the protein. We note that the spectral density is again Ohmic, with a cut-off frequency $\omega_p = 1/\tau_p$.

4.3 Model 3 - Static protein with no vacuum cavity

For a static protein with dielectric ϵ_p , we obtain

$$J_{pe}(\omega) = \frac{(\Delta\mu)^2}{2\pi\epsilon_0 b^3} \epsilon_p \frac{6(\epsilon_{e,s} - \epsilon_{e,i})}{(2\epsilon_{e,s} + \epsilon_p)(2\epsilon_{e,i} + \epsilon_p)} \frac{\omega\tau_{pe}}{\omega^2\tau_{pe}^2 + 1}, \quad (43)$$

$$\alpha_{pe} = \frac{(\Delta\mu)^2}{2\pi\epsilon_0 b^3} \epsilon_p \frac{6\tau_{pe}(\epsilon_{e,s} - \epsilon_{e,i})}{(2\epsilon_{e,s} + \epsilon_p)(2\epsilon_{e,i} + \epsilon_p)} \quad (44)$$

where $\epsilon_{e,s}$ and $\epsilon_{e,i}$ are the static and high frequency frequency dielectric constants of the environment respectively, and $\tau_{pe} = \frac{2\epsilon_{e,i} + \epsilon_p}{2\epsilon_{e,s} + \epsilon_p}\tau_{D,e}$ where $\tau_{D,e}$ is the Debye relaxation time of the solvent. We note that the spectral density is again Ohmic, with a cut-off frequency $\hbar\omega_{pe} \sim h/\tau_{pe}$.

4.4 Model 4 - Dynamic protein and dynamic solvent

The full spectral density (Model 4) describes the total coupling to the protein and solvent, but is too complex to be written analytically and because of the multiple timescales involved may be non-Ohmic. However, there are many cases where the use of one of the simpler descriptions (Models 1-3) would be preferable. For example if the dielectric of either the protein or solvent were not known, it would be useful to have a quick test of whether obtaining these parameters is worthwhile - if the protein contributes negligible coupling beyond pushing the solvent back to a new distance, then specially obtaining its dielectric through experiment or simulation would be pointless.

An even more compelling reason is that if either the solvent or the protein can be deemed unimportant, then simulations of the chromophores do not require their inclusion, saving valuable computational power. Conversely, if (for example) the solvent can be shown to have a significant effect on the chromophore, then treating the protein only will be insufficient and solvent effects must be included.

Therefore, we explore, in particular, under what conditions the protein dynamics may be neglected. The following discussion assumes that the dielectric relaxation time of the protein is longer than that of the solvent, which is expected to be true in the vast majority of cases. A similar calculation could be performed in the opposite limit, although we do not do so here. When both timescales are comparable, no simple method can determine the most important contribution.

4.4.1 Limit of a small chromophore surrounded by a large protein

In the case of an “infinite” protein $a/b \rightarrow 0$, the full spectral density (Model 4) reduces to $J_p(\omega)$ (the spectral density for Model 2)

$$J_p(\omega) = \frac{(\Delta\mu)^2}{4\pi\epsilon_0 a^3} \text{Im} \frac{2(\epsilon_p(\omega) - 1)}{2\epsilon_p(\omega) + 1} \quad (45)$$

In this limit, the solvent can be neglected when compared to the protein. We might naively assume then that, especially since the ratio a/b appears cubed, when the protein is several times larger than the chromophore the above spectral density can be used and the protein coupling far stronger than the solvent. However, a closer examination of (35) shows that if $\epsilon_p(\omega) \approx 1$, the solvent will be more significant even for large values of b/a , and a more appropriate expression for the spectral density describes the chromophore in a cavity of radius b surrounded by solvent.

Therefore, we seek a more precise statement for when the protein can be ignored. The full spectral density $J_{\text{full}}(\omega)$ can be rewritten:

$$J_{\text{full}}(\omega) = \frac{(\Delta\mu)^2}{2\pi\epsilon_0 a^3} \frac{\left(\frac{\epsilon_p+2}{2\epsilon_p+1}\right) \left(\frac{\epsilon_e-\epsilon_p}{2\epsilon_e+\epsilon_p}\right) \frac{a^3}{b^3} + \left(\frac{\epsilon_p-1}{2\epsilon_p+1}\right)}{\left(\frac{2(\epsilon_p-1)}{2\epsilon_p+1}\right) \left(\frac{\epsilon_e-\epsilon_p}{2\epsilon_e+\epsilon_p}\right) \frac{a^3}{b^3} + 1} \quad (46)$$

We can expand this expression in $\frac{\epsilon_e-\epsilon_p}{2\epsilon_e+\epsilon_p} \frac{a^3}{b^3}$. Note that although this is a complex quantity, provided both the real and imaginary parts are small compared to unity we can use the Taylor series expression $\frac{ax+b}{cx+1} \approx b + (a-bc)x$. Furthermore, both the real and imaginary parts of the prefactor of this expansion coefficient will be less than unity, and a sufficient condition for this expansion to be valid is that a/b be small. We find

$$\begin{aligned} J_{\text{full}}(\omega) &\approx J_p(\omega) + \frac{(\Delta\mu)^2}{2\pi\epsilon_0 b^3} \text{Im} \left[\frac{\epsilon_e(\omega) - \epsilon_p}{2\epsilon_e(\omega) + \epsilon_p} \right] \left(\frac{9\epsilon_p}{(2\epsilon_p + 1)^2} \right) \\ &= J_p(\omega) + J_s(\omega) \end{aligned} \quad (47)$$

where $J_s(\omega)$ represents the solvent contribution to the spectral density. Note that the dynamics of the protein only contribute to the first term, which conversely contains no reference to the solvent. The second term includes the

solvent dynamics plus the high frequency limit of the protein dielectric constant as the only relevant protein property. Therefore, we identify the first term with the protein contribution and the second term with the solvent, modified by the presence of the protein's high frequency dielectric.

4.4.2 Relevance of protein vs. solvent

By comparing the magnitudes of these two terms in (47), we can establish the relative importance of the solvent and protein over different frequency ranges. We might expect that around $\omega = 1/\tau_p$ and $\omega = 1/\tau_e$ that the protein and solvent contributions should dominate respectively. Therefore, there should be a cross over point where the two contributions are roughly equal, somewhere in the range $1/\tau_p \ll \omega \ll 1/\tau_e$, which is what we look for now.

As defined above, the cut-off frequency of $\omega_p = 1/\tau_p$. Assuming a Debye dielectric for the protein, eq. (41) can be approximated to first order in ω_p/ω as:

$$J_p(\omega) \approx \omega_p^2 \alpha_p / \omega, \quad \omega \gg \omega_p \quad (48)$$

Therefore, the tail end of the spectral densities given fall off as $1/\omega$ (as compared to their linear rise for $\omega \ll \omega_p$).

Noting that the reorganisation energy for this spectral density is $E_p = \alpha_p \omega_p$, we write the spectral density for $\omega \gg \omega_p$ as $J_p(\omega) = E_p \omega_p / \omega$. (This is quite different to the spectral density for $\omega \ll \omega_p$, which is $J(\omega) = E_p \omega / \omega_p$.)

The second term in (47) is somewhat more difficult to evaluate. We will again Taylor expand in $1/(\tau_p \omega)$. We note, however, that by extracting a factor of $1/a^3$ from both terms of (47) the second term is proportional to $(a/b)^3$, which we already assumed is "small" in the first Taylor expansion. Therefore, when we again Taylor expand around ω_p/ω we need only work to zeroth order so that our total final approximation for $J_{\text{full}}(\omega)$ is to first order in two expansion variables. This yields,

$$J_s(\omega) \approx \frac{9\epsilon_{p,i}}{(2\epsilon_{p,i} + 1)^2} J_{pe}(\omega) \quad (49)$$

where $J_{pe}(\omega)$ is the spectral density for Model 3, with $\epsilon_p \equiv \epsilon_{p,i}$, i.e., the chromophore inside a constant dielectric (high frequency) protein with no cavity, surrounded by the solvent. The solvent contribution is therefore Ohmic, with

$$\alpha_s = \frac{(\Delta\mu)^2}{2\pi\epsilon_0 b^3} \epsilon_p \frac{6\tau_s(\epsilon_{e,s} - \epsilon_{e,i})}{(2\epsilon_{e,s} + \epsilon_{p,i})(2\epsilon_{e,i} + \epsilon_{p,i})} \left(\frac{9\epsilon_{p,i}}{(2\epsilon_{p,i} + 1)^2} \right) \quad (50)$$

where $\epsilon_{e,s}$ and $\epsilon_{e,i}$ are the static and high frequency frequency dielectric constants of the environment respectively, and $\tau_s = \frac{2\epsilon_{e,i} + \epsilon_{p,i}}{2\epsilon_{e,s} + \epsilon_{p,i}} \tau_{D,e}$ where $\tau_{D,e}$ is the Debye relaxation time of the bulk solvent. Furthermore, since $\epsilon_{p,i}$ is of order one, the coefficient in (49) is also of order one, and roughly $\alpha_s \approx \alpha_{pe}$ (with an appropriate choice of ϵ_p).

Therefore, equating the two spectral densities suggests a cross over between solvent and protein dominance at frequency ω_{co} ,

$$\frac{\omega_{co}}{\omega_{pe}} = \sqrt{\frac{\alpha_p}{\alpha_s}} \quad (51)$$

This ratio is always much larger than one for typical values of dielectric constants and relaxation times. For frequencies above this limit, provided we are in the regime $b \gg a$, we would expect that the protein dynamics are irrelevant for the system, and the dynamics of the chromophore is "slaved" to the solvent fluctuations. Similar effects have been observed in enzyme kinetics [68]. At low frequencies ($\omega \ll \omega_{co}$), the protein dynamics dominate and the details of the solvent are mostly irrelevant. The relative contributions of the protein and solvent spectral densities are illustrated in Figure 6.

Hence, we expect that even when the chromophore is "shielded" from the solvent by the protein that the short time (0.1 psec) dynamics can still be dominated by the solvent. This raises questions about the recent assignment of the observed ultrafast solvation to protein dynamics [49, 50, 69].

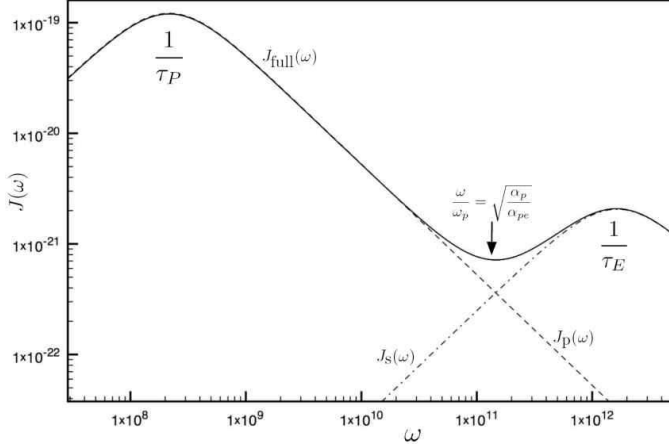


Figure 6: The relative importance of the solvent and protein dynamics for chromophores in large proteins. Log-log plot of the spectral density for Model 4 $J_{\text{full}}(\omega)$ (solid line) and its two contributions, the protein ($J_p(\omega)$, dashed line) and solvent ($J_s(\omega)$, dot-dash line) contributions. The frequency scale of the cross-over is as predicted by equation (51). Here, $b = 4a$, the solvent is water and the protein dielectric is $\epsilon_p^s = 6$, $\epsilon_p^i = 2.5$ and relaxation time $\tau_p = 10$ ns.

4.5 Model 5 - Bound water

Our goal is to obtain analytic criteria which tell us when and where the bound water is relevant. If the dielectric contribution of the bound water dominates over that of the protein, we can use Model 5 to describe the system. Instead of the chromophore pocket being treated as the cavity, now the entire protein is treated as a cavity of radius b with frequency-independent dielectric ϵ_p . This is surrounded by a shell of bound water with radius c (so the shell has width $c - b$) and dielectric $\epsilon_b(\omega)$ (with the subscript representing the bound water). We expect that the layer of bound water (typically [11] about 4.5 Å) will be thin compared to the rest of the protein ($b \sim 20$ Å), and so we are interested in the limit $b \approx c$. We simplify the spectral density (36) in the same way as Section 4.4, now Taylor expanding in $\frac{c-b}{b}$, which yields

$$J_5(\omega) \approx \frac{(\Delta\mu)^2}{2\pi\epsilon_0 b^3} \text{Im} \left[\frac{\epsilon_e - \epsilon_p}{2\epsilon_e + \epsilon_p} - \frac{3(2\epsilon_e + \epsilon_b)(\epsilon_e - \epsilon_b)}{\epsilon_b(2\epsilon_e + \epsilon_p)^2} \frac{(c-b)}{b} \right] \quad (52)$$

$$= J_{pe}(\omega) + J_{bw}(\omega) \quad (53)$$

The first term represents the spectral density of a chromophore inside a cavity of radius b with dielectric constant ϵ_p surrounded by a bulk solvent, and so is the spectral density in the absence of the bound water, as described by Model 3. The second term, which depends on the ratio $\frac{c-b}{b}$, a measure of the thickness of the bound water, can therefore be identified with the contribution to the spectral density of the bound water:

$$J_{bw}(\omega) = -\frac{2}{\epsilon_b} \left(\frac{2\epsilon_e + \epsilon_b}{2\epsilon_e + \epsilon_p} \right)^2 \left(\frac{\epsilon_e - \epsilon_b}{2\epsilon_e + \epsilon_b} \right) \frac{(c-b)}{b} \quad (54)$$

The $\frac{\epsilon_e - \epsilon_b}{2\epsilon_e + \epsilon_b}$ term represents a generalisation of Model 3 describing a chromophore inside a protein with radius b with the dielectric of the bound water, surrounded by the bulk solvent. Alone, this spectral density is unphysical, becoming

negative at low frequencies. However, in this context (and noting the preceding negative sign) we can interpret it as the bound water reducing the coupling to the environment at higher frequencies. If we consider frequencies much less than the bulk solvent relaxation time $1/\tau_e$, then we can consider the bulk solvent to be represented by its static dielectric $\epsilon_{e,s}$. Then, the bound water term can be expressed as

$$J_{bw}(\omega) \approx \frac{1}{(2\epsilon_e + \epsilon_p)^2} \text{Im} \left[\left(1 + \frac{2\epsilon_{e,s}}{\epsilon_b} \right) (\epsilon_b - \epsilon_{e,s}) \right] \quad (55)$$

$$= \frac{1}{(2\epsilon_e + \epsilon_p)^2} \left(1 + \frac{2\epsilon_{e,s}^2}{|\epsilon_b(\omega)|^2} \right) \text{Im} \epsilon_b(\omega) \quad (56)$$

Using a Debye form for the bound water spectral density, gives $\text{Im}[\epsilon_b(\omega)] = (\epsilon_{b,s} - \epsilon_{b,i}) \frac{\omega \tau_b}{1 + \omega^2 \tau_b^2}$. However, we must also include the $|\epsilon_b(\omega)|^2$ contribution to the frequency dependence. We find again that we have an Ohmic spectral density for the bound water contribution, with dimensionless coupling

$$\alpha_b = \frac{3(\Delta\mu)^2}{2\pi\epsilon_0 b^3} \left(\frac{c-b}{b} \right) \frac{(\epsilon_{b,s}^2 + 2\epsilon_{e,s}^2)(\epsilon_{b,s} - \epsilon_{b,i})}{\epsilon_{b,s}^2(2\epsilon_{e,s} + \epsilon_c)^2} \tau_b \quad (57)$$

In comparison with the solvent contribution,

$$\frac{\alpha_b}{\alpha_{pe}} \approx \left(\frac{c-b}{b} \right) \frac{\tau_b}{\tau_e} \frac{\epsilon_{b,s} - \epsilon_{b,i}}{\epsilon_{e,s} - \epsilon_{e,i}} \frac{(\epsilon_{b,s}^2 + 2\epsilon_{e,s}^2)(2\epsilon_{e,i} + \epsilon_p)}{\epsilon_{b,s}^2(2\epsilon_{e,s} + \epsilon_p)} \quad (58)$$

We would typically expect $\epsilon_{e,s} \gg \epsilon_{e,i}$, $\epsilon_{b,s} \gg \epsilon_{b,i}$, and $\epsilon_{e,s} \gg \epsilon_{b,s}$ and the cavity dielectric to be small compared to any static frequency, but perhaps comparable to the high frequency values of the bulk or bound water. Therefore,

$$\frac{\epsilon_{b,s} - \epsilon_{b,i}}{\epsilon_{e,s} - \epsilon_{e,i}} \frac{(\epsilon_{b,s}^2 + 2\epsilon_{e,s}^2)(2\epsilon_{e,i} + \epsilon_p)}{\epsilon_{b,s}^2(2\epsilon_{e,s} + \epsilon_p)} \approx \frac{\epsilon_{b,s}}{\epsilon_{e,s}} \frac{4\epsilon_{e,s}^2 \epsilon_{e,i}}{2\epsilon_{b,s}^2 \epsilon_{e,s}} \approx \frac{\epsilon_{b,i}}{\epsilon_{b,s}} \quad (59)$$

which we expect to be of order one. Therefore, we would usually expect

$$\frac{\alpha_b}{\alpha_{pe}} \sim \frac{c-b}{b} \frac{\tau_b}{\tau_{pe}} \quad (60)$$

Hence, if $\tau_b \gg \tau_{pe} \approx \tau_e$, as is observed [70, 71], then we would expect the bound water to be the dominant effect. Further, since the heights of the peaks are approximately given by their reorganisation energy ($J(\omega_c) = \alpha\omega_c \sim E_R$) we find

$$\frac{E_b}{E_{pe}} \approx \frac{c-b}{b} \quad (61)$$

where E_b, E_{pe} are the reorganisation energies of the bound water and solvent plus protein respectively. We might typically expect $\frac{c-b}{b} \approx 0.2$ [11], and so the bound water peak should be one fifth the height of the environment peak. However, the bound water term of $J_5(\omega)$ actually reduces the height of the solvent peak – shielding the chromophore from the higher frequency interactions of the environment – so the two peaks may in fact have comparable heights. The cross-over frequency between the bound water and bulk water contributions from the environment can again be determined by the condition $J_s(\omega) = J_b(\omega)$. Assuming that the bulk and bound water timescales are sufficiently separated that at the cross-over point $J_b(\omega)$ is in the decaying tail and $J_e(\omega)$ is in the linear region, then the cross-over frequency is given by

$$\frac{\omega_{co}}{\omega_b} = \sqrt{\frac{\alpha_{pe}}{\alpha_b}} \quad (62)$$

However, it should be noted that the bound water has a significant effect in reducing the coupling to the higher frequency modes, and so ignoring the bound water may produce incorrect predictions for the spectral density even well into the bulk solvent's frequency range.

5 Spectral densities determined from ultra-fast optical spectroscopy

The spectral function $J(\omega)$ associated with optical transitions in chromophores can be extracted from ultra-fast laser spectroscopy [72]. The time dependence of the Stokes shift in the fluorescence spectrum, where $\nu(t)$ is the maximum (or the first frequency moment) of the fluorescence spectrum at time t , can be normalised as

$$C(t) = \frac{\nu(t) - \nu(\infty)}{\nu(0) - \nu(\infty)} \quad (63)$$

such that $C(0) = 1$, and $C(\infty) = 0$ when the fluorescence maxima has reached its equilibrium value. This is related to the spectral density by

$$C(t) = \frac{\hbar}{E_R} \int_0^\infty \frac{J(\omega)}{\omega} \cos(\omega t) d\omega \quad (64)$$

where E_R is the total reorganisation energy given in eq. (23), which also equals half the total Stokes shift. This can be derived by taking the derivative of (18) with respect to time, since

$$\nu(t) = \epsilon - \frac{d\theta(t)}{dt}. \quad (65)$$

The function $C(t)$ is sometimes referred to as the hydration correlation function and experimental results are often fitted to several decaying exponentials,

$$C(t) = A_g \exp(-\frac{1}{2}(t/\tau_g)^2) + A_1 \exp(-t/\tau_1) + A_2 \exp(-t/\tau_2) + A_3 \exp(-t/\tau_3) + \dots \quad (66)$$

where $A_g + A_1 + A_2 + \dots = 1$. This corresponds to a form of the spectral density

$$J(\omega) = A_g \tau_g \sqrt{\frac{\pi}{2}} \exp[-(\omega \tau_g)^2/2] + \frac{\alpha_1 \omega}{1 + (\omega \tau_1)^2} + \frac{\alpha_2 \omega}{1 + (\omega \tau_2)^2} + \dots \quad (67)$$

where the dimensionless couplings α_j ($j = 1, 2, \dots$) are related to the total reorganisation energy by $\alpha_j = E_R A_j \tau_j$.

Of interest is the presence of a Gaussian component to the relaxation [73, 74] which is observed at short times, followed by exponential decays at long times. These features are predicted by the spin-boson model [75, 36], with a Gaussian relaxation on time scales of order $1/\omega_c$ and exponential decay through the Fermi Golden Rule for $t \gg 1/\omega_c$. See also the discussion at the end of Section 2. These issues have also been explored in quantum measurement theory in the context of continuous measurement and quantum Zeno effect [36].

Table 3 gives values of the fitting parameters (E_R, A_j, τ_j) determined by fast laser spectroscopy for a range of chromophores and different environments, both protein and solvent. We do not claim the list is exhaustive of all the published values, but is meant to be indicative. We note the following general features. (i) The total Stokes shift is large, showing that the chromophores interact strongly with their environment. (ii) The Stokes shift varies significantly between different environments, both solvent and protein. (iii) The different decay times observed for a particular system can vary by several orders of magnitude. (iv) Yet the relative contributions of the ultrafast (100's fsec) and slow (10's psec) response are often of the same order of magnitude.

Table 3: Solvation relaxation times for various chromophores in a range of environments. The values of relaxation times and their relative weights are determined by fitting the time dependence of the dynamic Stokes shift (63) or three-pulse photon echo peak shift (3PEPS) to the functional form (66). Some papers fit the data to (63) with $A_g = 0$. Note there is some variation in estimates of the reorganisation energy depending on whether one estimates it from the maxima in the absorption and emission spectra or from the first frequency moment of the spectra [11]. It should be noted that the time resolution is different in the various experiments. Some did not have access to femtosecond time scales and so we have left the relevant columns blank. SC is Subtilisin Carlsberg. HSA is Human serum albumin. In HSA the Acrylodan chromophore is at the surface of the protein, whereas the Phycocyanobilin chromophore is much less exposed to the solvent. HSA is in its native folded form in the buffer but denatures in concentrations of Gdn.HCl (guanidine hydrogen chloride) greater than about 5M. DCM is 4-(dicyanomethylene)-2-methyl-6-(p-dimethylaminostyryl) 4H-pyran, bR is bacteriorhodopsin, MPTS is 8-methoxypyrene-1,3,6-trisulfonate and bis-ANS is 1,1-bis(4-anilino)naphthalene-5,5' disulfonic acid.

Chromophore	Protein	Solvent	Ref.	E_R (cm $^{-1}$)	A_g, τ_g	A_1, τ_1	A_2, τ_2	A_3, τ_3
Eosin	none	water	[24]	877	0.73, 17 fsec	0.15, 400 fsec	0.12, 3 psec	
Eosin	lysozyme	water	[11]	710	0.7, 18 fsec	0.1, 310 fsec	0.1, 7 psec	
Trp	none	water	[76]			0.2, 180 fsec	0.8, 1 psec	
Trp	SC	water	[77]	1440		0.6, 800 fsec	0.4, 38 psec	
Trp	Rube	water	[76]			0.17, 1 psec	0.26, 12 psec	
Trp	Monellin	Buffer	[25]			0.46, 1.3 psec	0.54, 16 psec	0.57, 320 psec
Dansyl	SC	water	[77]	1180		0.94, 1.5 psec	0.06, 40 psec	
DCM	HSA	Tris buffer	[78]	515			0.25, 600 psec	0.75, 10 nsec
Prodan	none	buffer	[79]	2313		0.47, 130 fsec	0.53, 770 fsec	
Prodan	HSA	buffer	[79]	916		0.19, 780 fsec	0.56, 2.6 psec	0.25, 32 psec
Acrylodan	HSA	buffer	[79]	1680		0.23, 710 fsec	0.41, 3.7 psec	0.36, 57 psec
Acrylodan	HSA	0.2M Gdn.HCl	[79]			0.16, 280 fsec	0.36, 5.4 psec	0.48, 61 psec
Acrylodan	HSA	0.6M Gdn.HCl	[79]			0.2, 120 fsec	0.55, 2 psec	0.25, 13.5 psec
Coumarin 153	none	acetonitrile	[80]	2200		0.8, 100 fsec	0.2, 700 psec	
C343-peptide	Calmodulin	Water, buffer	[80]	250		0.9, 100 fsec	0.1, 2.4 psec	
Coumarin 343	none	water	[81]	1953	0.48, 25 fsec	0.2, 126 fsec	0.35, 880 fsec	
Phycocyanobilin	C-phycocyanin	buffer	[49]	372	0.5, 18 \pm 8 fsec	0.2, 100 \pm 30 fsec	0.2, 6 \pm 5 psec	
Phycocyanobilin	C-phycocyanin	buffer	[50]	372	0.9, 140 \pm 40 fsec		0.1, > 10 psec	
MPTS	none	buffer	[82]	2097		0.8, 20 fsec	0.2, 340 fsec	
MPTS	Ab6C8	buffer	[82]	1910		0.85, 33 fsec	0.1, 2 psec	0.05, 67 psec
bis-ANS	GlnRS (native)	water	[26]	750			0.45, 170 psec	0.55, 2.4 nsec
bis-ANS	GlnRS (molten)	urea	[26]	500			0.63, 60 psec	0.37, 0.96 nsec
4-AP	GlnRS (native)	water	[26]	1330			0.85, 40 psec	0.15, 580 psec
4-AP	GlnRS (molten)	urea	[26]	700			0.77, 50 psec	0.23, 0.9 nsec
Retinal	bR	buffer	[69]	1430	1, 50 fs			

In order to further elucidate the relationship between these experiments and our work we now consider a detailed comparison to one of the specific systems studied.

5.1 Eosin in Lysozyme

Three pulse photon echo spectroscopy can also be used to extract the spectral density, albeit indirectly. [11] This technique is analogous to stimulated spin echo measurements used in nuclear magnetic resonance to extract the phase relaxation time T_2 . The solvation dynamics of the fluorescein dye eosin bound to lysozyme in an aqueous solution was studied and compared to that for eosin in water without the protein[11]. For both systems, ultrafast solvation relaxation occurs in about 10 fsec and is assigned to bulk water. However, for the lysozyme-eosin complex a slower relaxation also occurred on the scale of 100 psec. This is assigned predominantly to water bound to the protein, mostly in the first hydration shell. This can be compared with dielectric dispersion measurements [83] which suggest that there are two solvation relaxation times of 4 and 270 psec. A molecular dynamics simulation of lysozyme in an explicit solvent environment of 5345 water molecules found a single solvation relaxation time of 100 psec [84]. Jordanides et al. [11] used the dynamic dielectric continuum model of Song and Chandler [85] to extract $J(\omega)$, based on four different dielectric models, similar to those considered by us. The full time dependence of the solvation was best described by a model which included the frequency dependence of dielectric constant of both the lysozyme and the water bound at the protein surface. These models for the lysozyme complex can be compared to our models if some simplifying assumptions are made. In particular, we need to treat the lysozyme protein as spherical with the eosin complex at its centre. Models I and II in Ref. [11] then correspond to our Models 3 and 5, respectively. Models III and IV are approximately our Model 4, with the appropriate choice for the protein dielectric constant of the protein. The

For comparison to Models II and III, we assume a cavity radius of $a = 22.5\text{\AA}$, corresponding to the radius of lysozyme and a protein radius of an additional 4.5\AA ($b = 27\text{\AA}$), which describes the bound water layers [11]. The bound water dielectric is taken to have a Debye frequency dependence with $\epsilon_{p,s} = 15$, $\epsilon_{p,i} = 2$, and $\tau_p = 1\text{ ns}$ since these are the dominant features of the dielectric constant shown in Figs. 3 and 4 of ref. [83] obtained from dielectric dispersion measurements on hydrated lysozyme powders. (Two main relaxation times are found, one at 20 ps and a spread of values at approximately 1 ns, however the 1 ns timescale dominates and allows us to apply the single Debye dielectric approximation.) The solvent is assumed to be water, and the change in dipole moment of eosin is assumed to be 8 Debye [24]. We find two peaks in the spectral density, in agreement with fig. 6 of Ref. [11], and their positions ($\omega = 0.1\text{cm}^{-1}, 1.8\text{cm}^{-1}$) are reasonably close to those found in experiment (c.f., $\omega = 0.02\text{ cm}^{-1}, 1\text{cm}^{-1}$). However, the amplitude of the spectral density in our model is about by two orders of magnitude smaller than was deduced in Ref. [11], (approximately 2cm^{-1} for our model, compared to 200cm^{-1}). This discrepancy is most likely because the eosin chromophore does not sit centrally in the protein, as shown in Figure 5 of [11], and so is more directly influenced by the solvent than we have taken into account. A more appropriate model in this case may be the eosin chromophore directly surrounded by the bound water surrounded by the solvent. This would significantly increase the coupling of the eosin to the environment.

For Model IV, we treat the eosin molecule as a vacuum cavity of radius $a = 2.25\text{\AA}$, inside the lysozyme with radius $b = 22.5$ (not including the surrounding bound water). In agreement with Figure 6 of Ref. [11] we see only a single peak, centred at approximately 0.05cm^{-1} , although the spectral density is too large by an order of magnitude. Finally, for Model I of ref. [11], we can apply Model 3 with a radius of $b = 22.5\text{\AA}$ corresponding to lysozyme, and choose the protein dielectric to have the static value $\epsilon_p = 2$. This model then produces a spectral density with a single peak at approximately 10cm^{-1} , which agrees roughly with the first peak of Model I in Figure 6 of Ref. [11], but is too small by two orders of magnitude. We do not see the additional peaks at higher frequencies. It should be pointed out that our models do not attempt to capture the the high frequency features of the spectral densities obtained in Ref. [11]. Such features would come from high frequency features of the dielectric functions.

6 Determining the spectral density from molecular dynamics simulations

For several specific proteins molecular dynamic simulations have been used to determine several quantities relevant to this work: the static dielectric constant of the protein, the frequency dependent dielectric constant, solvation dynamics, or the spectral density associated with an optical transition in a chromophore or an electron transfer. [86, 84, 63, 56, 87, 22, 88, 89, 23, 3, 90, 91, 92] We hope that our work will stimulate further simulations of the spectral density. To determine it one needs to determine time correlations of the (reaction field) electric field at the location of the chromophore (see Eqn. (30)) within the protein.

Equivalently, the spectral density can be related to the fluctuations in the energy difference between the ground and excited states of the system [88]. In terms of the Hamiltonian ((16)), the fluctuations are in the term which couples to σ_z , and which we denote $\delta V(t)$ (the shift ϵ is constant, so doesn't contribute to the fluctuations). It can be shown [40] that the spectral density is given by the Fourier transform of the fluctuation correlation function:

$$\frac{J(\omega)}{\omega} = \frac{1}{k_B T} \int_0^\infty dt \cos \omega t [\delta V(t) \delta V(0)]. \quad (68)$$

To obtain the spectral density, the fluctuations in the energy gap must be simulated for a sufficiently long time that the above integral converges for the frequency range of interest.

We now briefly review some of the results on specific proteins that are relevant to this paper.

6.1 Tryptophan in monellin and water

Molecular dynamics was used to calculate the time correlation function $S(t)$ for trajectories of a few nanoseconds [92]. For free Trp in bulk water $S(t)$ was fit to a bi-exponential decay function with $A_1 = 0.86 \pm 0.04$, $\tau_1 = 70 \pm 10$ fs, and $A_2 = 0.14 \pm 0.04$, $\tau_2 = 0.7 \pm 0.2$ ps. For Trp-3 in the protein monellin $S(t)$ was fit to a tri-exponential form with $A_1 = 0.66 \pm 0.02$, $\tau_1 = 70 \pm 10$ fs; $A_2 = 0.22 \pm 0.02$, $\tau_2 = 1.0 \pm 0.1$ ps; $A_3 = 0.12 \pm 0.01$, $\tau_3 = 23 \pm 2$ psec. The two faster decays were assigned to the bulk water and the slowest component ($\tau_3 = 23 \pm 2$ ps) was assigned to protein dynamics including the motion of the chromophore within the protein. This assignment is consistent with the interpretation of NMR measurements [93] but is different to that given in the associated experimental measurements [25] of the time dependent Stokes shift. The latter assigned the slower time scale (~ 20 psec) to the dynamic exchange between water bound at the protein surface (the first hydration shell) with bulk water.

6.2 Frequency dependent dielectric properties of an HIV1 zinc finger peptide in water

This peptide consisted of 18 amino acid residues and was simulated in a periodic box containing 2872 water molecules. [22] It was simulated for 13.1 nsec and exhibited a clear separation of time scales associated with dielectric relaxation of the different parts of the system. The water had a dielectric relaxation time of 7 psec, comparable to that for bulk water. Dielectric relaxation of the protein was dominated by a time scale of 4.3 nsec comparable to that found in simulations of other proteins and comparable to the time scale for rotation of the whole protein. The static dielectric constant of the peptide was estimated to be 15.

6.3 Frequency dependent dielectric properties of ubiquitin in water

Ubiquitin is a small globular protein composed of 76 amino acids. It was simulated in a cubic box containing 5523 water molecules for runs of 5 nsec duration. [23] Time dependent correlation functions could be fit to sums of two decaying exponentials with different weights and relaxation times. In the dielectric relaxation the three dominant timescales observed were 7 psec, 2.6 nsec, and 1.9 nsec. These were associated with the bulk water, with rotation of the whole protein, and the bound water and side chains at the protein surface, respectively.

6.4 Electron transfer in the *Rps. Viridis* reaction centre

Electron transfer in a biomolecule can be described by the spin-boson model (4)[41]. The spectral density associated with electron transfer in the reaction centre of the photosynthetic system *Rhodopseudomonas viridis* has been obtained from molecular dynamics simulations by two different research groups, using the energy gap correlation function method described above. Schulten and Tesch [94] modelled the protein over 40 ps using the available X-ray structure including 74 crystallised water molecules. The resulting spectral density [40] is ohmic, with coupling constant $\alpha = 25$ and a relaxation time of 94 fs (corresponding to a cut-off energy of $\hbar\omega_c = 7$ meV).

Simulations carried out at temperatures of 300 K and 80 K yielded similar spectral densities, supporting the temperature independence of the spectral density. Thus, provided the electron transfer matrix element, Δ in Eqn. (4), is small compared to $\hbar\omega_c$, we are in the parameter range considered by Ref. [33] and the electron transfer is in the regime of incoherent relaxation.

In Ref. [95], two models for the protein were used to calculate the correlation function. In model I, only the protein (again from the available X-ray structure) was included, while in model II the crystallisation water molecules and the detergent molecule were also included. The correlation function for both models exhibited an initial fast decay (50 fs for model I, 100 fs for model II), followed by a slow relaxation regime. The calculated spectral density for model I is approximately ohmic [96] with a relaxation time of 50 fs. For model II, the spectral density is more complicated, with a greater weighting on the lower frequencies. Small amplitude correlations were persistent on time scales longer than the decay time of 94 fs, found in Ref. [40]. The bulk solvent is not included in the simulations in either Ref. [95], nor Ref. [40]. The former argues based on experiments showing little dependency of electron transfer on temperature, that the environment probably has little effect on the electron transfer.

The results we obtained for the spectral densities from our continuum models can give some insight into the above results. First, the coupling α is so large, because of the large change in dipole moment associated with the electron transfer. We estimate a change in dipole moment of about $\Delta\mu = 17e\text{\AA} = 82\text{D}$, corresponding to an electron being transferred 17\text{\AA}, based on Fig. 2 of ref. [96]. We approximate the inner cavity inside the protein as $a \sim 9\text{\AA}$. The protein is assumed to have a high frequency dielectric constant $\epsilon_p^i \sim 2$ [18], although actual values may range between 1.5 – 2.5. Assuming an average radius of $b = 40\text{\AA}$ for the whole protein and including no solvent effects, we can fit the spectral density calculated in Ref. [40] to the spectral density to our Model 2 with $e_s = 3$ and $\tau_p = 100$ fs. However, it is hard to justify such a short protein relaxation time unless the electron transfer is coupling to vibrations of covalently bonded atoms within the protein. In agreement with the experimental observations mentioned above, we find that the inclusion of a solvent (e.g., using our Model 4) in our continuum model has little effect on the environmental coupling for parameter values relevant to this system.

7 Conclusion

The focus of this paper has been on the coupling of optical transitions in biological chromophores to their environment. However, as was done in the previous section, the approach and results presented here can be readily adapted to other transitions involving two quantum states which differ in the value of their electric dipole moment. Examples include intersystem crossing, electron and proton transfer. Indeed, we have recently used this approach to estimate the friction associated with proton transfer in enzymes.[97]

We hope our work will stimulate more work considering the following general claims, which this paper has elucidated.

(i) The most realistic and reliable approach to modelling quantum dynamics in specific biomolecular systems is in terms of “minimal” models such as the spin-boson model where the system parameters and spectral density are extracted from experiment and/or quantum chemistry and molecular dynamics.

(ii) Even when the active site of a protein is shielded from bulk water, the latter can still have a significant effect

on the quantum dynamics of the active site, especially if the time scale of interest is comparable to the solvation time scale associated with the bulk water. This can lead to solvent fluctuations dominating protein dynamics and function [68].

(iii) The environment of the active site can be divided into three distinct components, the surrounding protein, water at the protein surface, and bulk water. The times scales associated with the dielectric relaxation of each usually differs by several orders of magnitude and so each makes a unique contribution the coupling of the quantum dynamics of the active site to the environment. Furthermore, the relative importance (relevance) of each component depends on the time scale of interest in the quantum dynamics.

8 Acknowledgements

This work was supported by the Australian Research Council. We thank Paul Burn, Jacques Bothma, Paul Curni, Paul Davies, Ken Ghiggino, Hugh McKenzie, Paul Meredith, Gerard Milburn, Seth Olsen, Ben Powell, Jeff Reimers, Jenny Riesz, Maximilian Schlosshauer, Greg Scholes, and Thomas Simonson for very helpful discussions.

References

- [1] Helms, V. *Curr. Opinion Struct. Bio.* **2002**, *12*, 169.
- [2] Sarikaya, M.; Tamerler, C.; Jen, A. K.-Y.; Schulten, K.; Baneyx, F. *Nature Materials* **2003**, *270*, 577.
- [3] Warshel, A.; Parson, W. W. *Quart. Rev. Biophys.* **2001**, *34*, 563.
- [4] Gilmore, J.; McKenzie, R. *Chem. Phys. Lett.* **2006**, *421*, 266.
- [5] Gilmore, J.; McKenzie, R. *J. Phys.: Cond. Matt.* **2005**, *17*, 1735.
- [6] Edsall, J.; McKenzie, H. *Adv. Biophys.* **1983**, *16*, 53.
- [7] Mattos, C. *Trends in Biochem. Sci.* **2002**, *27*, 203.
- [8] Wand, A. *Nature Struct. Bio.* **2001**, *8*, 926.
- [9] Davies, P. C. W. *BioSystems* **2004**, *78*, 69.
- [10] Hahn, S.; Stock, G. *J. Phys. Chem. B* **2000**, *104*, 1146.
- [11] Jordanides, X. J.; Lang, M. J.; Song, X.; Fleming, G. R. *J. Phys. Chem. B* **1999**, *103*, 7995.
- [12] Chattoraj, M.; King, B. A.; Bublitz, G. U.; Boxer, S. G. *Proc. Natl. Acad. Sci.* **1996**, *93*, 8362.
- [13] Fleming, G.; van Grondelle, R. *Physics Today* **1994**, *47*(2), 48.
- [14] Chachisvilis, M.; Kühn, O.; Pullerits, T.; Sundström, V. *J. Phys. Chem. B* **1997**, *101*, 7275.
- [15] Trinkunas, G.; Herek, J. L.; Polívka, T.; Sundström, V.; Pullerits, T. *Phys. Rev. Lett.* **2001**, *86*, 4167.
- [16] Hu, X.; Ritz, T.; Damjanovic, A.; Schulten, K. *J. Phys. Chem. B* **1997**, *101*, 3854.
- [17] Pullerits, T.; Chachisvili, M.; Sundström, V. *J. Phys. Chem.* **1996**, *100*, 10792.

- [18] Monshouwer, R.; Abrahamsson, M.; van Mourik, F.; van Grondelle, R. *J. Phys. Chem. B* **1997**, *101*, 7241.
- [19] Genick, U.; Soltis, S.; Kuhn, P.; Canestrelli, I.; Getzoff, E. *Nature* **1998**, *392*, 206.
- [20] van Holde, K. E.; Johnson, W. C.; Ho, P. S. *Physical Biochemistry*; Prentice-Hall, 1998.
- [21] Afsar, M. N.; Hasted, J. B. *Infrared Phys.* **1978**, *18*, 835.
- [22] Löffler, G.; Schreiber, H.; Steinhäuser, O. *J. Mol. Biol.* **1997**, *270*, 520.
- [23] Boresch, S.; Höchtl, P.; Steinhäuser, O. *J. Phys. Chem. B* **2000**, *104*, 8743.
- [24] Lang, M. S.; Jordanides, X. J.; Song, X.; Fleming, G. *J. Chem. Phys.* **1999**, *110*, 5884.
- [25] Peon, J.; Pal, S. K.; Zewail, A. H. *Proc. Natl. Acad. Sci.* **2002**, *99*, 10964.
- [26] Sen, P.; Mukherjee, S.; Dutta, P.; Halder, A.; Mandal, D.; Banerjee, R.; Roy, S.; Bhattacharyya, K. *J. Phys. Chem. B* **2003**, *107*, 14563.
- [27] Zhang, L. Y.; Friesner, R. A. *Proc. Natl. Acad. Sci.* **1998**, *95*, 13603.
- [28] Kawatsu, T.; Kakitani, T.; Yamato, T. *J. Phys. Chem. B* **2002**, *106*, 11356.
- [29] Borgis, D.; Hynes, J. T. *J. Phys. Chem.* **1996**, *100*, 1118.
- [30] Ben-Nun, M.; Molnar, F.; Lu, H.; Phillips, J. C.; Martínez, T. J.; Schulten, K. *Faraday Discuss.* **1998**, *110*, 447.
- [31] Weiss, U. *Quantum dissipative systems*; World Scientific: Singapore, 2nd ed., 1999.
- [32] Joos, E.; Zeh, H. D.; Kiefer, C.; Kupsch, J.; Stamatescu, I. O. *Decoherence and the Appearance of a Classical World in Quantum Theory*; Springer, 2nd ed., 2003.
- [33] Leggett, A.; Chakravarty, S.; Dorsey, A.; Fisher, M.; Garg, A.; Zwerger, W. *Rev. Mod. Phys.* **1987**, *59*, 1.
- [34] Prokof'ev, N.; Stamp, P. *Rep. Prog. Phys.* **2000**, *63*, 669.
- [35] Lesage, F.; Saleur, H. *Phys. Rev. Lett.* **1998**, *80*, 4370.
- [36] Joos, E. *Phys. Rev. D* **1984**, *29*, 1626.
- [37] Carmeli, B.; Chandler, D. *J. Chem. Phys.* **1988**, *89*, 452.
- [38] Muhlbacher, L.; Egger, R. *J. Chem. Phys.* **2003**, *118*, 179.
- [39] Bulla, R.; Lee, H.-J.; Tong, N.-H.; Vojta, M. *Phys. Rev. B* **2005**, *71*, 045122.
- [40] Xu, D.; Schulten, K. *Chem. Phys.* **1994**, *182*, 91.
- [41] Garg, A.; Onuchic, J. N.; Ambegaokar, V. *J. Chem. Phys.* **1985**, *83*, 4491.
- [42] Hettich, C.; Schmitt, C.; Zitzmann, J.; Kühn, S.; Gerhardt, I.; Sandoghdar, V. *Science* **2002**, *298*, 385.
- [43] Kühn, O.; Sundström, V.; Pullerits, T. *Chem. Phys.* **2002**, *275*, 15.

- [44] Niimura, N.; Arai, S.; Kurihara, K.; Chatake, T.; Tanaka, I.; Bau, R. In Niimura, N., Mizuno, H., Helliwell, J. R., Westhof, E., Eds., *Hydrogen- and Hydration-Sensitive Structural Biology*, page 17, 2005.
- [45] Pal, S. K.; Peon, J.; Zewail, A. H. *Proc. Natl. Acad. Sci.* **2002**, *99*, 1763.
- [46] Grant, E.; Sheppard, R.; South, G. *Dielectric behavior of biological molecules*; Oxford: Clarendon, 1978.
- [47] Nandi, N.; Bagchi, B. *J. Phys. Chem. B* **1997**, *101*, 10954.
- [48] Bhattacharyya, K. *Acc. Chem. Res.* **2003**, *36*, 95.
- [49] Homoelle, B. J.; Edington, M. D.; Diffey, W. M.; Beck, W. F. J. *J. Phys. Chem. B* **1998**, *102*, 3044.
- [50] Riter, R. E.; Edington, M. D.; Beck, W. F. *J. Phys. Chem. B* **1996**, *100*, 14198.
- [51] Mahan, G. D. *Many-Particle Physics*; Plenum Press: New York and London, 2nd ed., 1990.
- [52] Onsager, L. *J. Am. Chem. Soc.* **1936**, *58*, 1486.
- [53] Bottcher, C. *Theory of electric polarization*, Vol. v.1; Elsevier: Amsterdam, 1973.
- [54] Reina, J. H.; Quiroga, L.; Johnson, N. F. *Phys. Rev. A* **2002**, *65*, 032326.
- [55] Unruh, W. G. *Phys. Rev. A* **1995**, *51*, 992.
- [56] Höfinger, S.; Simonson, T. *J. Comp. Chem.* **2001**, *22*, 290.
- [57] Voges, D.; Karshikoff, A. *J. Chem. Phys.* **1998**, *108*, 2219.
- [58] Schutz, C.; Warshel, A. *PROTEINS: Structure, Function, and Genetics* **2001**, *44*, 400.
- [59] Hsu, C.-P.; Song, X.; Marcus, R. A. *J. Phys. Chem. B* **1997**, *101*, 2546.
- [60] Song, X.; Marcus, R. *J. Chem. Phys.* **1993**, *99*, 7768.
- [61] Horng, M. L.; Gardecki, J. A.; Papazyan, A.; Maroncelli, M. *J. Phys. Chem.* **1995**, *99*, 17311.
- [62] Kindt, J. T.; Schmuttenmaer, C. A. *J. Phys. Chem.* **1996**, *100*, 10373.
- [63] Pitera, J.; Falta, M.; van Gunsteren, W. F. *Biophysical Journal* **2001**, *80*, 2546.
- [64] Moog, R. S.; Kiki, A.; Fayer, M.; Boxer, S. G. *Biochemistry* **1984**, *23*, 1546.
- [65] Trissl, H.-W.; Bernhardt, K.; Lapin, M. *Biochemistry* **2001**, *40*, 5290.
- [66] Pal, S.; Balasubramanian, S.; Bagchi, B. *J. Chem. Phys.* **2004**, *120*, 1912.
- [67] Pierce, W.; Boxer, S. G. *J. Phys. Chem.* **1992**, *96*, 5560.
- [68] Fenimore, P.; Frauenfelder, H.; McMahon, B.; Parak, F. G. *Proc. Natl. Acad. Sci.* **2002**, *99*, 16047.
- [69] Kennis, J. T. M.; Larsen, D. S.; Ohta, K.; Facciotti, M. T.; Galeser, R. M.; Fleming, G. R. *J. Phys. Chem. B* **2002**, *106*, 6067.
- [70] Bagchi, B. *Annu. Rep. Prog. Chem., Sect C* **2003**, *99*, 127.

- [71] Yoshiба, K.; Терамото, А.; Накамуре, Н.; Шиката, Т.; Мицухаси, Й.; Сорай, М.; Хаяши, Й.; Миура, Н. *Biomacromolecules* **2004**, *5*, 2137.
- [72] Fleming, G.; Cho, M. *Annu. Rev. Phys. Chem.* **1996**, *47*, 109.
- [73] Stratt, R. M.; Cho, M. *J. Chem. Phys.* **1994**, *100*, 6700.
- [74] Jimenez, R.; Salazar, G.; Jina, Y.; Hoo, T.; Romesberg, F. E. *Proc. Natl. Acad. Sci.* **2004**, *101*, 3803.
- [75] Hwang, H.; Rossky, P. H. *J. Chem. Phys.* **2004**, *120*, 11380.
- [76] Zhong, D.; Pal, S. K.; Zhang, D.; Chan, S. I.; Zewail, A. H. *Proc. Natl. Acad. Sci.* **2002**, *99*, 13.
- [77] Pal, S. K.; Peon, J.; Zewail, A. H. *Proc. Natl. Acad. Sci.* **2002**, *99*, 15297.
- [78] Pal, S. K.; Mandal, D.; Sukul, D.; Sen, S.; Bhattacharyya, K. *J. Phys. Chem. B* **2001**, *105*, 1438.
- [79] Kamal, J. K. A.; Zhao, L.; Zewail, A. H. *Proc. Natl. Acad. Sci.* **2004**, *101*, 13411.
- [80] Changenet-Barret, P.; Choma, C.; Gooding, E.; DeGrado, W.; Hochstrasser, R. *J. Phys. Chem. B* **2000**, *104*, 9322.
- [81] Jimenez, R.; Fleming, G.; Kumar, P.; Maroncelli, M. *Nature* **1994**, *369*, 471.
- [82] Jimenez, R.; Case, D.; Romesberg, F. *J. Phys. Chem. B* **2002**, *106*, 1090.
- [83] Harvey, S. C.; Hoekstra, P. *J. Phys. Chem.* **1972**, *76*, 2987.
- [84] Smith, P.; Brunne, R.; Mark, A.; Gunsteren, W. V. *J. Phys. Chem.* **1993**, *97*, 2009.
- [85] Song, X.; Chandler, D. *J. Chem. Phys.* **1998**, *108*, 2594.
- [86] King, G.; Lee, F. S.; Warshel, A. *J. Chem. Phys.* **1991**, *95*, 4366.
- [87] Simonson, T.; Perahia, D. *Proc. Natl. Acad. Sci.* **1995**, *92*, 1082.
- [88] Xu, D.; Schulten, K. In *The Photosynthetic Bacterial Reaction Center: II. Structure, Spectroscopy and Dynamics*; Breton, J., Vermeglio, A., Eds.; Plenum Press, 1992; page 301.
- [89] Kosztin, I.; Schulten, K. In *Molecular dynamics methods for bioelectronic systems in photosynthesis*; Aartsma, T., Matysik, J., Eds.; Kluwer Academic Publishers, in press.
- [90] Miyashita, O.; Go, N. *J. Phys. Chem. B* **2000**, *104*, 7516.
- [91] Rudas, T.; Schröder, C.; Boresch, S.; Steinhauser, O. *J. Chem. Phys.* **2006**, *124*, 234908.
- [92] Nilsson, L.; Halle, B. *Proc. Natl. Acad. Sci.* **2005**, *102*, 13867.
- [93] Halle, B. *Philos. Trans. R. Soc. London B* **2004**, *359*, 1207.
- [94] Schulten, K.; Tesch, M. *Chem. Phys.* **1991**, *158*, 421.
- [95] Marchi, M.; Golden, J. N.; Chandler, D.; Newtons, M. *J. Am. Chem. Soc.* **1193**, *115*, 4178.
- [96] Makri, N.; Sim, E.; Makarov, D. E.; Topaler, M. *Proc. Natl. Acad. Sci.* **1996**, *93*, 3926.
- [97] Quantum tunneling of hydrogen species in enzymes: A minimal model. Bothma, J. B. Sc. (Hons.) Thesis, University of Queensland (unpublished), **June 2006**.